Green Chemistry

PERSPECTIVE

View Article Online
View Journal | View Issue

Cite this: *Green Chem.*, 2024, **26**, 5127

Ionic liquid-stabilized metal oxoclusters: from design to catalytic application

Yunxiang Qiao, †[a] Enting Shi,†[b] Xinjia Wei[b] and Zhenshan Hou *[b]

Metal oxoclusters constitute a dynamic and expanding domain of research with versatile applications in catalysis, materials science, medicine, and beyond. Particular attention has been given to their potential utility due to their distinctive properties. The incorporation of ionic liquid (IL) environments into metal oxocluster (MOC) systems offers numerous advantages, including higher stability, tunable coordination to metal sites, and the capability to dissolve diverse substrates for catalytic applications. Although IL-stabilized MOCs (IL–MOCs) are still in the developmental phase, their potential to revolutionize catalysis is substantial. As research progresses, IL–MOCs will likely play an increasingly important role in catalysis. This perspective article focuses on the preparation methods of IL–MOCs, how the MOCs are stabilized/regulated by ILs or even PIL (polymeric ILs), as well as their catalytic applications, including oxidation, epoxidation, oxidative desulfurization, biomass oxidation, hydroxylation of benzene, acid catalysis, CO_2 activation and utilization, carbonylation, hydrogenation/hydrolysis, electrochemistry, *etc*. IL–MOCs have played a crucial role in the development of sustainable chemistry in the light of the potential opportunities and challenges. The unique advantages make IL–MOCs outstanding candidates for industrial catalysts.

Received 29th January 2024,
Accepted 3rd April 2024

DOI: 10.1039/d4gc00515e

rsc.li/greenchem

1. Introduction

Metal oxoclusters (MOCs) are a diverse and fascinating class of inorganic compounds composed of metal atoms (typically transition metals) bonded to oxygen atoms. These clusters can be found in nature, but they can also be synthesized in the laboratory. Characterized as molecular oxide species, MOCs have discrete chemical formulas and can be isolated as pure compounds. They are soluble in water or some organic solvents and have a wide range of compositions and structures, shapes and sizes, and are composed of a wide range of different metal cations. Distinguished by their unique structures and properties, MOCs can be tailored for a wide range of specific applications, including catalysis,[1] materials science,[2–4] and biomedical applications.[5,6] In catalysis, they are able to serve as catalysts in practical processes like the production of fuels and fine chemicals.[7] Moreover, MOCs are under investigation as potential materials for batteries, solar cells, and other electronic devices in materials science.[8] Additionally, they have shown to have antiviral, antibacterial, and anticancer activity, expanding their potential applications in the biomedical field.[9,10] In summary, MOCs offer versatility in terms of their compositions and structures, making them highly adaptable for specific applications across different scientific and technological domains.

Common examples of MOCs include polyoxometalates (POMs), MOCs with organic ligands (*e.g.* ILs) or metalloenzymes *etc*. POMs, a specific class of MOCs, are composed of early transition metals, such as molybdenum, tungsten, and vanadium, in their highest oxidation states.[11–13] Various POM structures have been determined, with the most known ones being the Keggin, Dawson, Anderson, Lindqvist, Siverton and Wauth structures, *etc*. (Fig. 1). For instance, Keggin-POM clusters, featuring 12 metal atoms and 40 oxygen atoms, while Lindqvist-POM clusters, comprising 6 metal atoms and 18

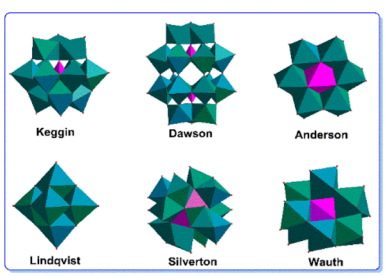

Fig. 1 Representation of the classical structures of polyoxometalates.

[a]*Max-Planck-Institut für Kohlenforschung, Kaiser-Wilhelm-Platz 1, 45470 Mülheim an der Ruhr, Germany*
[b]*State Key Laboratory of Green Chemical Engineering and Industrial Catalysis, Research Institute of Industrial Catalysis, School of Chemistry & Molecular Engineering, East China University of Science and Technology, Shanghai 200237, People's Republic of China. E-mail: houzhenshan@ecust.edu.cn; Tel: +86 21 64251686*
† These authors contributed equally to this work.

oxygen atoms, both show a cage-like structure and share similar applications.

On the other hand, ionic liquids (ILs) are a class of non-volatile, non-flammable, and tunable solvents, which are made up of ions. They can be tailored to have specific properties, such as polarity, viscosity, and acidity, making them unique media for a wide variety of catalytic reactions and the synthesis of a wide range of MOCs. IL-stabilized MOCs (IL–MOCs) are a new class of catalysts that have shown great promise for a variety of applications in catalysis, electrochemistry, energy production, and materials science.[14–17] One of the key advantages of IL–MOCs is their high catalytic activity. This is due to the unique structure of these catalysts with the presence of the exposed metal sites, which allows for close contact between the highly exposed metal atoms and the reactants, thus facilitating the transfer of electrons and the formation of chemical bonds, which are essential for catalysis. ILs could not only stabilize MOCs, but also regulate MOCs through a combination of interactions, *e.g.* ionic and electrostatic forces, tuning of hydrophilicity or hydrophobicity, and facilitating redox processes. The careful selection of IL components and design considerations can tailor the IL environment to enhance the stability and catalytic properties of MOCs in catalytic applications.

Several research groups actively work on the use of IL–MOCs. In recent years, our group not only designed different IL–MOCs (especially POM-based ILs, POM–ILs), but also utilized them for catalytic epoxidation, oxidation, esterification, and carbonylation/carboxylation, *etc*. This perspective article aims to provide a brief overview of the development and catalytic applications of IL–MOCs, with a focus on the reports from our own research group and recent contributions from the other groups. Herein, we also briefly discuss the advantages, opportunities, challenges, and the developmental direction of IL–MOCs for the catalytic applications.

2. The synthesis routes for IL–MOCs

The synthesis of IL–MOCs involves the combination of MOCs with ILs.[17–19] It's essential to consider factors such as solubility, stability, and compatibility between the MOC and IL during the synthesis process. Additionally, the choice of synthesis method depends on the properties desired for the IL–MOC hybrids and the nature of the MOC and IL involved, and it can in turn influence the structure and properties of the resulting IL–MOCs. The general synthesis approaches of IL–MOCs mainly include ion exchange, direct mixing or dissolution, *in situ* synthesis, self-assembly strategy, *etc*.

2.1 Ion exchange

The ion exchange method for IL–MOC synthesis involves subjecting a preformed IL to ion exchange with a MOC anion, which replaces some or all of the counterions in the IL, resulting in the formation of IL–MOCs with MOC as the anion of the new IL. This simple method just consists of mixing the MOC (normally dissolved in water) with the organic salt dissolved in water or in a miscible organic solvent (often an alcohol) in the right stoichiometry. After a certain time of reaction whilst stirring, the two phases are separated sometimes with the help of centrifugation when emulsions are obtained. The heavy phase is normally the IL–MOC product which precipitates or forms a new liquid phase. After several times of washing, the resulting IL–MOC hybrids are dried and analyzed. As a typical example, the first reported POM–IL was prepared through partial exchange of the protons in heteropoly acid (HPA) by polyethylene glycol (PEG)-containing quaternary ammonium, yielding a liquid derivative of the POM with similar properties to other ILs (Scheme 1), such as a low melting point, comparable viscosity, and high conductivity.[20]

The more widely researched examples are the anion-exchange of PILs by POM anions, a process similar to that of monomeric ILs, except the cation is PIL.[21–23] PILs are the polymeric products of IL monomers, composed of polymeric backbones with IL species in each repeating unit, forming a network structure.[24] Mixing a PIL solution in a miscible organic solvent (often ethanol) with a MOC aqueous solution forms the desired PIL–MOC, which can be separated normally by filtration. As such, PIL–MOCs in this article refer to MOCs serving as anions of PILs. PILs exhibit properties similar to traditional ILs but possess additional characteristics stemming from their polymeric nature. These materials often feature high thermal stability, tunable mechanical properties, compatibility with various solvents and substrates, and more easily tunable amphiphilicity, *etc*. These characteristics make them similar to, but slightly different from monomeric IL–MOCs. PIL–MOCs are also widely used in various catalytic reactions, which is illustrated in the following sections.

2.2 Direct mixing or dissolution

This is a straightforward method where metal oxides are mixed or dissolved directly in an IL. The choice of IL depends on the desired properties of the resulting IL–MOCs. A specific example is the usage of protonated betaine bis(trifluoromethylsulfonyl)imide [Hbet][NTf_2] as a versatile task-specific IL that can be used for the selective solubilization of metal oxides and metal salts due to its acidic functional groups.[25,26] The zwitterionic nature of the betaine ligand in combination with the weakly coordination ability of $[NTf_2]^-$ anion facilitates the formation of metal complexes into oligonuclear and polynuclear metal complexes. Crystal structures of six metal complexes, cobalt(II), nickel(II), manganese(II), zinc(II), silver(I), and lead(II) compounds, were obtained after solubilizing metal oxides in [Hbet][NTf_2] in the presence of water.[26] The resulting crystals exhibited rich structural chemistry, including trimeric units for the cobalt(II) compound, tetrameric units for the manga-

$$H_3PW_{12}O_{40} + xS^+Cl^- \longrightarrow H_{3-x}S_x\,PW_{12}O_{40} + xHCl$$

$$S^+ = (CH_3)(C_{18}H_{37})N^+[(CH_2CH_2O)_nH][(CH_2CH_2O)_mH],\ m+n=15$$

Scheme 1 The synthesis of liquid salts by ion exchange.

nese(II) and zinc(II) compounds, pentameric units for the nickel(II), an oxo–hydroxo-cluster formation for the lead(II) compound, and polymeric units for the silver(I) compound.

2.3 *In situ* generation

MOCs can be generated *in situ* within an IL. The addition of a metal salt and a suitable oxidizing agent to an IL leads to the formation of MOCs within the IL medium, in which ILs act as both solvents and charge-compensating species. Noticeably, the reaction temperature can be increased further owing to the unique characteristics of ILs as high thermal stability and nearly non-volatility. The first member of a new family of POM–ILs, demonstrated by Rickert *et al.*,[27,28] was prepared by pairing Keggin or Lindqvist POM anions with tetraalkylphosphonium cations. Other examples are: $[EMIm]_4[[beta]\text{-}Mo_8O_{26}]$ (EMIm is 1-ethyl-3-methylimidazolium) could be obtained from the IL $[EMIm]BF_4$,[29] $[EMIm]_8Na_9[WFe_9(\mu_3\text{-}O)_3(\mu_2\text{-}OH)_6O_4H_2O(SiW_9O_{34})_3]\cdot 7H_2O$ and $[EMIm]_4[SiMo_{12}O_{40}]\cdot 12H_2O$ could be successfully produced in the IL [EMIM]Br.[30] Additionally, crystal-phase polyoxomolybdate compounds such as $[BMIm]_3NH_4[Mo_8O_{26}]$, $[BMIm]_4[PMo^{V}Mo_{11}O_{40}]$ and $[BMIm]_3[PMo_{12}O_{40}]$ (BMIm = 1-butyl-3-methylimidazolium) were synthesized *in situ* using $[BMIm][BF_4]$ and simple molybdate salts.[31] Detailed information on these *in situ* synthesis examples is shown in Table 1.

2.4 Self-assembly strategy

The self-assembly strategy of IL–MOC involves the spontaneous arrangement of MOCs within an IL environment, which is also known as amphiphile self-assembly media.[32–34] This process is governed by the specific interactions between the MOC anions and the IL cations, *e.g.* covalent and non-covalent (electrostatic, hydrophobic and solvophobic) interactions.[35] The same principle also applied to PILs, taking composite POM/PIL/Gr as an example, it is with monodisperse POM clusters immobilized by PIL been successfully supported on graphene (Gr) through ionic self-assembly (Fig. 2).[36] This synthesized composite shares a similar morphology to the original graphene, with POM anionic clusters being monodispersed on graphene, which endowed the catalyst with a higher specific surface area, large mesopore size, and dramatically improved accessibility of POMs. PILs play the linking role in bonding with POMs *via* multivalent electrostatic interactions and combining with graphene through a series of non-covalent interactions. The reason why self-assembly may occur is due to the multi-charged PIL cations and POM anions, which attracted each other because of opposite charges and resulted in the compact aggregations, as well as the highly negative-charged graphene surface under non-acidic conditions. Notably, neither the precise control nor toxic organic solvent were necessary for this process.

3. How the MOCs are stabilized/regulated by ILs

MOCs are a broad class of inorganic compounds with nano-sized dimensions. However, they can be unstable and prone to degradation. Thus the stabilization of MOCs is essential to prevent their aggregation and maintain their unique properties for various applications, which often involves careful control over the synthesis, as well as the use of compatible solvents,

Table 1 Examples of *in situ* synthesis of IL–MOCs

IL–MOCs	POM precursor	IL	*T*/°C	*t*	Ref.
$(R_3R'P)_2W_6O_{19}$	Na_2WO_4	$R_3R'PBr$	—	—	27 and 28
$[EMIm]_4[\beta\text{-}Mo_8O_{26}]$	$Na_2MoO_4\cdot 2H_2O$	$[EMIm]BF_4$	170	24 h	29
$[EMIm]_8Na_9[WFe_9(\mu_3\text{-}O)_3(\mu_2\text{-}OH)_6O_4H_2O(SiW_9O_{34})_3]\cdot 7H_2O$	$Na_{10}[SiW_9O_{34}]\cdot 16H_2O$, $Fe(NO_3)_3\cdot 9H_2O$	[EMIm]Br	150	Three days	30
$[EMIm]_4[SiMo_{12}O_{40}]\cdot 12H_2O$	$Na_2MoO_4\cdot 2H_2O$, $Na_2SiO_3\cdot 9H_2O$	[EMIM]Br	150	Three days	30
$[BMIm]_3NH_4[Mo_8O_{26}]$ (crystal)	Ammonium molybdate, $La(OH)_3$, 2-pyridinecarboxylic acid	$[BMIm][BF_4]$	140	Six days	31
$[BMIm]_4[PMo^{V}Mo_{11}O_{40}]$ (crystal)	$(NH_4)_6Mo_7O_{24}\cdot 4H_2O$, $La(OH)_3$, $NH_4H_2PO_4$	$[BMIm][BF_4]$	135	Six days	31
$[BMIm]_3[PMo_{12}O_{40}]$ (crystal)	Sodium molybdate, copper chloride, phosphoric acid, water	$[BMIm][BF_4]$	150	Seven days	31

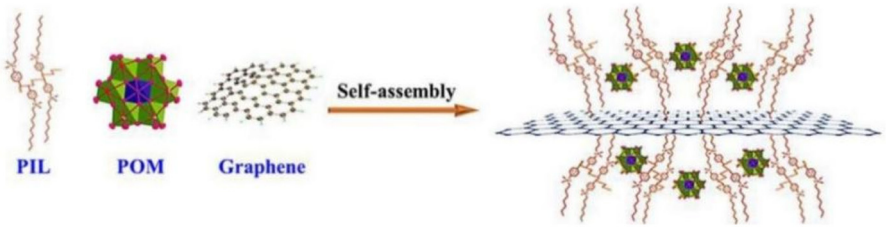

Fig. 2 Schematic diagram of preparation principle to the POM/PIL/Gr hybrids. Adapted from ref. 36 with permission from Elsevier, copyright 2020.

counterions,[37] ligands,[38] support materials[39] or surface modifications.[40] ILs have proved to be able to stabilize a wide range of MOCs *via* the following ways.

One way is by forming hybrids with MOCs that act directly as ILs' anions.[17] The unique combination of IL cations and MOC anions can be used to tune the activity and selectivity of IL–MOC/PIL–MOC catalysts. This type of hybrids is the focus of this perspective article, especially their design and catalytic application under green chemistry conditions (Scheme 2A).

Another way is by forming strong bonds with the metal atoms.[41–43] ILs are composed of cations and anions. The specific charge distribution on IL components can interact with charged sites on MOCs through electrostatic forces, and also their polar functional groups, such as nitrogen, oxygen, and sulfur atoms. This coordination can help to protect the MOCs from the environment, strengthen the bonds within the MOCs, and make them more stable, thus preventing them from decomposition (Scheme 2B).

To some extent, the universal solvent property of ILs can be ascribed to the strong bonds formed between the ILs and MOCs. So-called task-specific ILs, which are ILs with a functional group covalently tethered to the cation or anion, are being developed to increase the solubility of metal compounds in these solvents. The functional group that has the ability to coordinate with the metal ion, preferably as a bidentate or a polydentate ligand, facilitates the dissolution of MOCs. Taking deprotonated betaine $Me_3N^+CH_2COO^-$ as an example, the carboxylate group on one end of the molecule can act as a bridging ligand providing super-exchange pathways between metal ions, while the large trimethylammonium part on the other end behaves like a spacer that can separate adjacent chains.[26] And the protonated betaine (also called betainium) exhibits a higher acidity (pK_a 1.83) than alkanoic acids like acetic acid (pK_a 4.75) or propionic acid (pK_a 4.87), it is the higher acidity of the betainium ion improved an enhanced solubilizing ability for MOCs.

Yet another way is ILs can dissolve MOCs that are insoluble in traditional solvents and prevent them from aggregating.[44–46] ILs have the ability to dissolve a wide range of compounds, polar and non-polar, which is why they are often referred to as "universal solvents." This ability to dissolve a wide range of compounds makes ILs ideal for stabilizing MOCs, which can be quite complex and diverse in their structure and composition. Thus, ILs can provide a solvation environment that prevents the MOCs from aggregating and further improves the stability of the cluster (Scheme 2C).

Overall, ILs could stabilize the MOCs through ionic or electronic interactions, or by solubilization. In a sense, ILs could also regulate the stability and structural integrity as well as the catalytic activity of the MOCs within the IL environment. On one hand, ILs can be tailored to have varying degrees of hydrophilicity or hydrophobicity by selecting specific cation and anion combinations. This allows for the adjustment of the IL environment to match the hydrophilic or hydrophobic nature of MOCs, optimizing their interactions. On the other hand, ILs with appropriate structures can enhance the accessibility of catalytic active sites on MOCs. The unique architecture of ILs can act as a scaffold, providing an environment that facilitates interactions between reactants and the catalytic centers of MOCs. Furthermore, ILs often exhibit unique thermophysical properties, such as low volatility and high thermal stability. These characteristics can create a stable environment for MOCs, influencing their behavior, especially in high-temperature or high-pressure catalytic reactions.

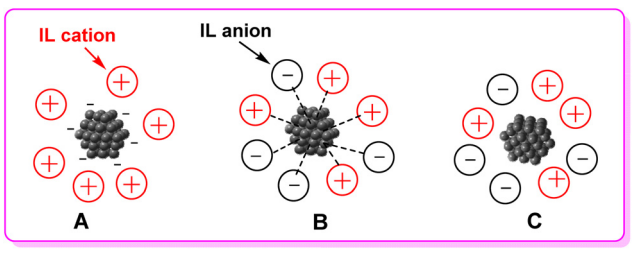

Scheme 2 MOCs are stabilized by ILs *via* different approaches: (A) the direct combination of IL cations and MOC anions; (B) the chemical bonds between IL ions and the metal atoms; (C) the solvation of MOCs in ILs.

4. Classification of IL–MOCs

IL–MOCs can be categorized based on their metal oxide compositions and structural arrangements. In the following, we will briefly introduce (1) peroxometalate anion-based (W, Nb, Ta, V, Ti *etc.*) ILs, (2) POM anion-based ILs, including Keggin and Lindqvist structure POM-based ILs, (3) a specific category of POM–ILs: POM–IL-anchored single-atom catalysts, and (4) another distinct category of POM–ILs: supported POM–IL. Table 2 provides examples of IL–MOCs, illustrating their diverse applications and structural characteristics.

4.1 Peroxometalate anion-based ILs

The investigation on peroxotungstate anion-based ILs represents an early research area of POM anion-based ILs. For instance, the combination of tungsten peroxo complex and imidazolium cation, with[49,50] or without[47,48] bidentate picolinato ligand, has been extensively studied and proved to be efficient catalysts for different chemical transformations.

Peroxoniobates, a noteworthy class of MOC materials, have gained attention for their structural diversity and high nucleophilicity, making them promising catalyst candidates for environment-friendly applications.[97] Consequently, a series of Nb-based ILs have been constructed in Hou's group, such as niobium peroxides modified with IL-type 1-dodecyl-3-methylimidazolium hydroxide,[55] the first proposed novel Nb-based IL, assigned as $[A^+][Nb{=}O(O{-}O)(OH)_2]$ (A^+ = ammonium cation),[56] and a series of Nb-based ILs coordinated by organic carboxylic acid,[57] and then a new class of carboxylate ILs-stabilized Nb oxoclusters[58] were reported. Moreover, Nb oxoclusters can also be stabilized/modified by readily available organic fluoride salts.[59] Furthermore, supramolecular com-

Table 2 Some examples of IL–MOCs

Type of MOCs	IL–MOCs	Application	Ref.
Peroxotungstate anion-based IL	$[HDIm]_2[\{W{=}O(O_2)_2\}_2(\mu\text{–}O)]$	Epoxidation	47
	MNP-$[HDMIM]_2[W_2O_{11}]$, MNP-$[SDMIM]_2[W_2O_{11}]$	Epoxidation	48
	Imidazolium–tungsten peroxo complex	Oxidative desulfurization	49 and 50
	$[BPy]_4W_{10}O_{32}$, $[BMIm]_4W_{10}O_{32}$	Alcohol oxidation	51
	$(P_{6,6,6,14})_4[W_{10}O_{32}]$	Olefin/alcohol oxidation	52 and 53
	$(P_{6,6,6,14})_4[W_{10}O_{32}]$	Selenoether oxidation	54
Peroxoniobate anion-based ILs	$[DMIm]_{0.1}{\cdot}Nb_2O_7{\cdot}2H_2O$; $[TTA]_{0.08}{\cdot}Nb_2O_7{\cdot}2H_2O$.	Epoxidation	55
	$[A^+][Nb{=}O(O\text{–}O)(OH)_2]$ (A^+ = ammonium cation)	Epoxidation	56
	[TBA][$NbO(OH)_2$(R)] (TBA = tetrabutylammonium; R = lactic acid, glycolic acid, malic acid)	Epoxidation	57
	[TBA][LA]-stabilized Nb oxoclusters	Epoxidation & sulfide oxidation	58
	Nb-OC@TBAF-0.5	Epoxidation	59
	18-Crown-6 and ammonium peroxoniobate (NH_4–Nb)	Epoxidation	60
Peroxotantalum anion-based ILs	$[P_{4,4,4,n}]_3[Ta(O)_3(\eta\text{-}O_2)]$, $P_{4,4,4,n}$ = quaternary phosphonium cation, n = 4, 8, and 14	Epoxidation	61
	$[P_{4,4,4,4}]_3[Ta(\eta^2\text{-}O_2)_3(CO_4)]$	Epoxidation	62
Peroxovanadium anion-based ILs	([TBA][Pic])-stabilized vanadium oxo-clusters (Pic = picolinate ions)	Alkane oxidation	63
	[BIm][Pic](Bim = 1-butylimidazolium)-stabilized vanadium oxo-cluster	Selective oxidative cleavage of β-O-4 lignin model compounds	64
Peroxotitanium anion-based ILs	Ti oxo-HSO_4	Oxidative desulfurization	65
Keggin structure POM-based IL	[PEG-containing quaternary ammonium][$PW_{12}O_{40}$]	Electrochemistry	20
	[Tetraalkylphosphonium] Keggin	Electrochemistry	27 and 28
	$[MIMPS]_3[PW_{12}O_{40}]$, $[PyPS]_3[PW_{12}O_{40}]$, $[TEAPS]_3[PW_{12}O_{40}]$	Esterification	66
	$[BMIm]_3[PW_{12}O_{40}]$	Epoxidation	67
	$[Dopy]_3[PW_{12}O_{40}]$	Epoxidation	68
	$[DEDSA]_3[PW_{12}O_{40}]$ $[DEDSA]_3[PMo_{12}O_{40}]$	Oxidation of alcohols	69
	Chiral IL-$[PW_{12}O_{40}]$	Asymmetric oxidation	70
	$[Im\text{-}PEG\text{-}Im]_{1.5}[PW_{12}O_{40}]$	Oxidation of benzyl alcohol	71
	$[Im\text{-}PEG\text{-}Im][HPW_{12}O_{40}]$	Esterification	72
	$[Im\text{-}PEG\text{-}Im]_{1.5}[PO_4(W(O)(O_2)_2)_4]$	Epoxidation	73
	$[BMIm]_3[PO_4(W(O)(O_2)_2)_4]$	Oxidation of alcohols	74
	Ni[MIMPSH][$PW_{12}O_{40}$]	Acetalization of benzaldehyde with ethylene glycol	75
	$[n\text{-}C_{16}H_{33}N\text{-}(CH_3)_3]_4Na_3PW_{11}O_{39}$	Epoxidation	76
	$[C_{12}MIm]_5PTiW_{11}O_{40}$, $[CTA]_5PTiW_{11}O_{40}$, $[TBA]_5PTiW_{11}O_{40}$	Epoxidation	77
	$(ODA)_4PMo_{11}VO_{40}$	Oxidation of benzyl alcohol	78
	$[MIMPS]_NH_{4-N}PMo_{11}VO_{40}$ (N = 1–4), $[PyPS]_3HPMo_{11}VO_{40}$, $[TEAPS]_3HPMo_{11}VO_{40}$, and $[BMIm]_3HPMo_{11}VO_{40}$	Cellulose into formic acid	79
	$[HC_4Im]_3PMo_{12}O_{40}$, $[HC_4Im]_5PV_2Mo_{10}O_{40}$, $[HC_2Im]_5PV_2Mo_{10}O_{40}$, $[HC_4Im]_4SiMo_{12}O_{40}$	Lignin depolymerization	80
	$[PyBS]_5PV_2Mo_{10}O_{40}$	Cellobiose to formic acid and levulinic acid	81
	Pyridinium cation-$PMo_{10}V_2O_{40}$	Alkane oxidation	82
	$[BMIm]_4[Ti(H_2O)TiMo_{11}O_{39}]$	Degradation of polyethylene terephthalate	83
	$[BMIm]_4[Ti(H_2O)TiMo_{11}O_{39}]$	Transesterification	84
	Co_4PW–PDDVAC (a porous POM-based composite)	Isolation of proteinase K	85
Lindqvist structure	[Tetraalkylphosphonium] Lindqvist	Electrochemistry	28
	$[TBA]_2Mo_6O_{19}$ and $[TBA]_2W_6O_{19}$	Electrolytes	86
	$[^t$Bu-Hptz$]_2[Mo_6O_{19}]$	Epoxidation	87
POM–IL-anchored single-atom	$[(n\text{-}C_4H_9)_4N]_6[SiW_{11}O_{39}Pd]$, $[(n\text{-}C_4H_9)_4N]_5[PW_{11}O_{39}Pd]$	Hydrocarboxylation of olefins	88
	$[TOMA_6SiW_{11}O_{39}Ru(dmso)]$, TOMA = methyltrioctylammonium	N-Formylation of amines with CO_2 and H_2	89
Supported POM–IL	$[\alpha\text{-}PW_{12}O_{40}]^{3-}$ immobilized on IL-modified polystyrene resin beads (PS–IL–PW)	Alcohol oxidation	90
	$[PW_{12}O_{40}]^{3-}$ immobilized on dual amino-functionalized IL-modified MIL-101(Cr)	Alcohol oxidation	91
	PEG–PW_{11}–CMC (carboxymethyl cellulose)	Epoxidation	92
	P_8W_{48}@PIL–G	Electrocatalysts	93 and 94
	AILs/POM/UiO-66-2COOH	Esterification	95
	$PMo_{10}V_2$-ILs@MIL-100(Fe)	Epoxidation	96

plexations between 18-crown-6 and ammonium peroxoniobate can lead to the supramolecular IL catalysts with suitable hydrophobicity by a direct mixing of 18-crown-6 and NH_4–Nb ($(NH_4)_3[Nb(O_2)_4]$) in methanol, which provides a much simpler approach, as compared with that of the previous Nb-based ILs.[60]

Hou's group also pioneered the development of early examples of ILs based on monomeric peroxotantalate anions.[61] Similar to other active POM–ILs, the Ta-based ILs ($[P_{4,4,4,n}]_3[Ta(O)_3(\eta\text{-}O_2)]$, $P_{4,4,4,n}$ = quaternary phosphonium cation, n = 4, 8, and 14) underwent a structural transformation in the presence of H_2O_2. Pressurization of $[P_{4,4,4,4}]_3[Ta(O)_3(\eta^2\text{-}O_2)]$ with CO_2 in the presence of H_2O_2 produced a new class of Ta-based peroxocarbonate IL ($[P_{4,4,4,4}]_3[Ta(\eta^2\text{-}O_2)_3(CO_4)]$), which was found to be more superior towards epoxidation to the monomeric peroxotantalate analogs, and the transformation between Ta-peroxocarbonate and peroxotantalate anions was completely reversible, leading to an excellent regeneration of IL catalysts.[62]

Vanadium oxoclusters have been synthesized through the condensation of peroxovanadium species in the presence of the functionalized IL [TBA][Pic] (TBA = tetrabutylammonium; Pic = picolinate ions) with tunable IL/V molar ratios.[63] Similarly, imidazolium IL [BIm][Pic] (BIm = 1-butyl-imidazolium)-stabilized vanadium oxocluster catalysts were prepared as well.[64]

Ti oxoclusters stabilized by carboxylic acid-functionalized imidazolium-based IL were also fabricated *via* a solvothermal method.[65] Characterization indicated that Ti oxoclusters (Ti oxo-HSO_4) existed in the form of subnanosized structure, uniformly dispersed with an average particle size of *ca.* 1 nm due to the protection role of the ILs. It was found that the coordination of the carboxylic acid functional group of IL with Ti sites could prevent the Ti oxo-HSO_4 from aggregation, and on the other hand, HSO_4^- could play an additional role in stabilizing the subnanosized Ti oxo-HSO_4 cluster *via* electrostatic interaction.

4.2 POM anion-based IL

The Keggin structure, characterized by α-Keggin anions with a general formula of $[XM_{12}O_{40}]^{n-}$, represents a prominent form for HPAs, where X is the heteroatom, M is the addendum atom (typically Mo or W), and O denotes oxygen. Self-assembling in acidic aqueous solutions, the Keggin structure is widely employed in POM catalysts. The first POM–IL hybrid, prepared *via* ion exchange method as illustrated in Section 2.1, is composed of a PEG-containing quaternary ammonium cation and 12-tungstophosphoric anion.[20] Subsequently, a series of POM–ILs with $PW_{12}O_{40}^{3-}$ anion but with different cations, such as pyridinium, phosphonium, ammonium, imidazolium, PEG-containing alkylimidazolium, and even chiral ILs were reported.[66–71] Partial exchange of the protons in $H_3PW_{12}O_{40}$ by a PEG-2000 chain-functionalized alkylimidazolium chloride yielded acidic [IM-PEG-IM][$HPW_{12}O_{40}$].[72] Furthermore, complexes pairing the $[PO_4(W(O)(O_2)_2)_4]^{3-}$ anion, the well-known and most important active species in Ishii–Venturello system, with imidazolium cations were reported as well.[73,74]

A series of transition-metal (M = Mn, Fe, Co, Ni, Cu) ion-exchanged $H_3PW_{12}O_{40}$-based IL catalysts were synthesized by integrating metal and methylimidazolium propyl sulfobetaine (MIMPS) zwitterionic IL precursors onto $H_3PW_{12}O_{40}$.[75] Hybrids comprising a lacunary-type phosphotungstate anion $[PW_{11}O_{39}]^{7-}$ and (PEG-containing) ammonium cations were also investigated.[76] Additionally, Ti-substituted POMs ($[C_{12}MIm]_5PTiW_{11}O_{40}$, $[CTA]_5PTiW_{11}O_{40}$, and $[TBA]_5PTiW_{11}O_{40}$) were synthesized and characterized.[77] Keggin type $H_5PV_2Mo_{10}O_{40}$ and $H_4PVMo_{11}O_{40}$-based POM–ILs were investigated as well due to their wide and high catalytic activity.[78,79,81]

Combining a Keggin $[PW_{12}O_{40}]^{3-}$ (or Lindqvist ($[W_6O_{19}]^{2-}$)) anion with an appropriate tetraalkylphosphonium can produce POM-based ILs, exhibiting comparable conductivity and viscosity to a previously described inorganic–organic POM–IL hybrid but possess enhanced thermal stability.[28] Furthermore, $[TBTP]_4PW_{11}VO_{40}$ and $[TBTP]_4PMo_{11}VO_{40}$ (TBTP = tributyl-tradecylphosphonium), composed of Keggin POMs and tetraalkylphosphonium cation have been synthesized.[98] They show layered structures due to the self-assembly of cations and anions through electrostatic interactions and van der Waals forces, and especially they also display reversible phase transformation process below 100 °C. It was indicated that the oxidability of the Mo-containing POM is greater than that of the W-containing analog from the electrochemical study, which provides valuable insight into the further development of POM–ILs.

4.3 POM–IL-single atom catalysts (POM–IL–SACs)

The concept of single-atom catalysts (SACs) is highly regarded within heterogeneous catalysis due to their ability to achieve maximum metal utilization. POMs with precisely known composition and structure, as well as a limited number of sites to anchor atomically dispersed metals, are reported to be good support material, and the resulting POM-supported SACs (POM–SACs) serve as valuable models for investigating the complex catalytic systems at the atomic level,[89–92,99] facilitating *in situ* spectroscopic studies of single atom sites during reactions. Moreover, they contribute to a deeper understanding of the structure–activity relationship and the dynamic changes in active sites during catalysis. POM clusters play a dual role as ligands and supports in the precise construction of SACs, enabling control over coordination states and active site loading. Additionally, the integration of ILs could help to isolate and stabilize SACs on solid support materials through interactions. Thus, POM–IL–SACs function as a hybrid catalyst, exhibiting catalytic activity akin to that of single-atom catalysts, while benefiting from the advantages of both homogeneous and heterogeneous catalysis.

Besides recent advancements in POM–SACs, several POM–IL–SACs systems were reported also in Hou's group, such as POM–IL–Rh SAC,[100] POM–IL Pd SAC,[88] and POM–IL–Ru SAC[89] catalytic systems. In these materials, the isolated single metal

atoms were proved to be incorporated into the POM structure according to analysis. The bulky IL cations, on one hand, function as stabilizers of the single atoms and thus avoid the usage of the organic phosphine ligands; on the other hand, they prevent the aggregation and leaching of the isolated metal atoms. These POM–IL–SACs displayed a unique "pseudo-liquid-phase" behavior and showed efficient activity for catalytic carbonylation reactions. The detailed discussion of Rh-catalyzed hydroformylation to produce aldehydes, Pd-catalyzed hydrocarboxylation to yield carboxylic acids, and Ru-catalyzed *N*-formylation of CO_2 to generate *N*-formyl compounds will be given in Section 5.4.

4.4 Supported POM–IL hybrids

Based on the recognized advantages of POM–ILs, it is anticipated that the self-assembly of POM–ILs on certain support materials would yield robust hybrids with enhanced chemical properties. IL-modified polystyrene resin beads proved to be a suitable support for POM.[90] Zhang and Keita *et al.* demonstrated the functionalization of graphene with POMs associated with PIL objects.[93,94] The one-pot synthesis of the P_8W_{48} ($[H_7P_8W_{48}O_{184}]^{33-}$)@PIL–graphene tri-component hybrids was performed by visible light irradiation of a mixture of the desired amounts of P_8W_{48} and PIL in the presence of graphite oxide. The P_8W_{48} serves as both an efficient graphite oxide reductant and a stabilizer. Due to the strong adsorption of P_8W_{48} on the resulting graphene sheets, water-dispersible P_8W_{48}@graphene hybrids were obtained without the need for surfactant or polymeric stabilizers. On the other hand, metal–organic frameworks (MOFs), which are inorganic–organic hybrid porous crystalline materials, were incorporated with POM–ILs due to their large surface area, highly-ordered structure, regular and accessible pores, as well as versatile architecture.[95,96] For instance, $H_3PW_{12}O_{40}$ could be immobilized into the nanocages of a dual amino-functionalized IL-modified MIL-101(Cr) framework under mild conditions.[91] UiO-66-2COOH MOFs were also functionalized with Keggin-type POM acids and further incorporated with sulfonated acidic ILs by pairing POM anions with functionalized IL cations.[95] Furthermore, a series of ILs-functionalized POM-based MOF hybrids (POMs–ILs@MOFs) *via* encapsulating ILs within POMs@MOFs were reported.[96] According to characterizations, POMs were successfully immobilized in MOF cages, with the structure of MOFs retained after immobilization.

5. The catalytic application of IL–MOCs

MOCs are widely recognized for their superior catalytic efficiency in both academic and industrial sectors compared to traditional homogeneous catalysts. The selection of an appropriate IL and its specific properties is crucial, considering the characteristics of MOCs and the intended application. It is imperative to verify the stability and compatibility of the IL with the clusters through comprehensive experimentation and characterizations. ILs provide a versatile and effective method for stabilizing MOCs in diverse research and industrial applications. The following outlines specific examples of IL–MOCs for catalytic applications.

5.1 The catalytic oxidation

Selective or partial oxidation of organic compounds is one of the most important chemical processes due to its industrial significance.[101] Since conventional oxidation reaction often suffers from challenges in achieving selective oxidation, leading to the formation of undesired by-products and reduced overall efficiency, selectively producing the specific products is both challenging and crucial. The application of IL–MOCs to oxidation catalysis is inspired by their attractive properties, such as adjustable structure, acidity and redox properties, inherent resistance to oxidative decomposition, high thermal and chemical stability, *etc*.

5.1.1 Olefin oxidation. Olefin oxidation can convert olefins into other products containing oxygen functionalities, such as diols, or carbonyl compounds, depending on the reaction conditions and the nature of the oxidizing agent. IL–MOC with the chemical formula $(P_{6,6,6,14})_4[W_{10}O_{32}]$ could be used as both solvent and catalyst for the catalytic oxidation of various alcohols and alkenes in the presence of H_2O_2 due to its good fluidity when the temperature increased and its very low dielectric constant comparable with those obtained for apolar organic solvents.[52] POM, which has no distinct stereoselectivity itself, could catalyze the asymmetric styrene oxidation with H_2O_2.[70] A series of chiral ILs, derived from optically pure *S*-nicotine with different alkyl lengths, were combined with the $PW_{12}O_{40}^{3-}$ anion. These hybrids showed synergistic advantages between POM and chiral ILs, resulting in complete conversion of styrene and a relatively high selectivity for *R*-(−)-1-phenylethane-1,2-diol with 72% yield and 96% enantiomeric excess under mild reaction conditions (Fig. 3). Notably, the chiral ILs function as chiral selectors for enantio-recognition and enhance the stereoselective potency of POMs.

5.1.2 Olefin epoxidation. As a distinct subset of olefin oxidation, olefin epoxidation has been extensively investigated using IL–MOCs as catalysts and will be discussed separately. Olefin epoxidation is a chemical process that involves the transfer of an oxygen atom from a peroxy compound (H_2O_2 is the most common one) to an olefin. IL–MOCs have been extensively studied for olefin epoxidation under mild reaction con-

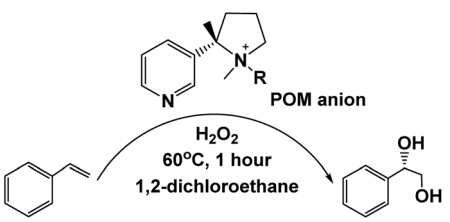

Fig. 3 The combination of the POM with the chiral IL for the asymmetric styrene oxidation with H_2O_2. Adapted from ref. 70 with permission from Elsevier, copyright 2020.

ditions, in which the POM facilitates the transfer of oxygen atoms to the olefin substrate, leading to the formation of epoxide products, while ILs not only stabilize the POM but also contribute to the overall catalytic performance through their unique properties, such as high thermal stability and tunable coordination environments.[67,68] The synergistic effects arising from the combination of POMs and ILs result in catalytic systems with improved efficiency and selectivity.

Various IL–MOCs, such as peroxotungstate anion- and Keggin structure-based POM–ILs, have shown particular efficiency in catalyzing the epoxidation of olefins. Most of them show reaction-induced phase-separation properties with the system transitioning from a tri-phase to an emulsion and eventually self-precipitating at the reaction's end, facilitating catalyst recovery and reuse.[73] To better reuse the hybrid material, the POM–ILs could be immobilized on support materials to get magnetically separable catalysts exhibiting constant activity over at least ten cycles in the epoxidation of olefins with H_2O_2.[48]

Ti-substituted POMs ($[C_{12}mim]_5PTiW_{11}O_{40}$, $[CTA]_5PTiW_{11}O_{40}$, and $[TBA]_5PTiW_{11}O_{40}$) were also efficient for catalyzing the epoxidation of various olefins and the heterogeneous nature of catalysis in ethyl acetate media was confirmed by a hot catalyst filtration test.[77] It was found the organic countercations significantly affected the catalytic activity, and the stable Ti-based peroxo structure serves as the active species, allowing for multiple catalytic runs without notable loss of activity.

Similar high activity also applies to polyoxoniobate-based POM–ILs. Niobium peroxides modified with IL-type 1-dodecyl-3-methylimidazolium hydroxide demonstrated excellent yields (80–99%) for the epoxidation of allylic alcohols to their epoxides even if the reaction was performed without any other solvent under ice bath conditions.[55] The first proposed novel Nb-based POM–IL, designated as $[A^+][Nb{=}O(O{-}O)(OH)_2]$ (A^+ = ammonium cation), showed excellent catalytic activity and recyclability in epoxidizing various allyl alcohols under solvent-free, ice bath conditions using H_2O_2 as the oxidant.[56] It was observed that the formation of an $[Nb(O{-}O)_2(OOH)_2]^-$ active center promoted the whole reaction through a homogeneous process and also facilitated the recyclability. To broaden the substrate scope from allyl alcohols to more challenging-to-convert olefins, a series of Nb-based POM–ILs coordinated by organic carboxylic acids were designed.[57] Subsequently, a new class of carboxylate ILs-stabilized Nb oxoclusters was reported.[58] They had an average particle size of 2–3 nm and exhibited extremely high catalytic activity for the epoxidation of olefins and allyl alcohols, using only 50 ppm of catalyst (0.065 mol%), with turnover number (TON) values exceeding 1000, outperforming the same transition metal catalyst (Scheme 3). Furthermore, organic fluoride salts were found to be able to stabilize or modify Nb oxoclusters due to their strong coordination interaction with Nb sites.[59] The F atoms also form a hydrogen-bond interaction with the –OH group of the allylic alcohol, favoring the epoxidation reaction. Notably, the supramolecular complexations between

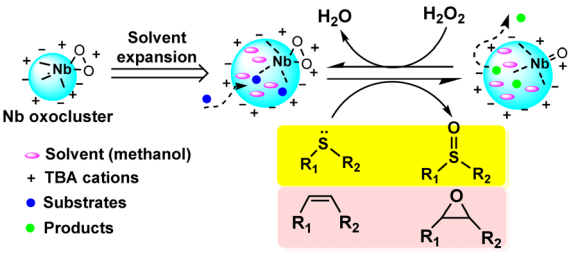

Scheme 3 The proposed reaction route for selective oxidation of sulfides and olefins with IL-stabilized Nb oxocluster catalysts. Adapted from ref. 58 with permission from Wiley-VCH Verlag GmbH, Weinheim, copyright 2019.

ammonium peroxoniobate and 18-crown-6 were designed, demonstrating high catalytic activity and recyclability for olefin epoxidation.[60] These supramolecular IL catalysts provide easy access to hydrophobic substrates and represent a novel approach to selective olefin epoxidation.

Recently, the Lindqvist-type POM $[t$Bu-Hptz$]_2[Mo_6O_{19}]$ (tBu-Hptz = 2-*tert*-butyl-5-(2-pyridyl)tetrazole) was studied as epoxidation catalysts using readily available and relatively eco-friendly hydroperoxide oxidants (hydrogen peroxide and *tert*-butyl hydroperoxide).[87] This POM acted as a homogeneous catalyst and could be recycled by employing an IL solvent. It was found that the type of anion of the IL could affect the catalytic performance. Besides, the presence of water in the ILs (in different amounts) is often unavoidable, which may also influence the level of hydration of the anions, the strength of the anion–cation interactions, and the viscosity of the IL medium. On the other hand, one cannot exclude the possibility that ion-exchange might occur between $[t$Bu-Hptz$]_2[Mo_6O_{19}]$ and the IL, depending on the type of IL.

Meanwhile, the POM-supported IL@core–shell polymer nanoparticles (PS–ImC_n–PW_4) have been established to offer an efficient Pickering emulsion catalytic system (Scheme 4).[102] A series of PS–ImC_n–PW_4 nanospheres were prepared with cross-linked polystyrene as the core and POM–IL as the shell. Allyl chloride and H_2O_2 can be emulsified by these nanospheres. The surface properties of the nanospheres can be modulated by changing the carbon chain length of IL, which in turn affects the properties and catalytic performance of the Pickering emulsion. Interestingly, C_2–C_6 can stabilize O/W-type emulsion, while C_8–C_{12} refers to W/O-type emulsion. This catalytic system can be used for the epoxidation of allyl chloride with low-concentration (9.6 wt%) H_2O_2 under solvent-free conditions.

Overall, the effectiveness of POM–IL-catalyzed epoxidation reactions stems from the cooperative interactions between POMs and ILs, enabling a catalytic system that is efficient, selective, and environmentally friendly.

5.1.3 Alkane oxidation. Oxidation of alkanes to aldehydes, ketones, and carboxylic acids is a challenging reaction due to the relatively unreactive nature of alkanes.[95] However, IL–MOCs can overcome this challenge by providing a highly active

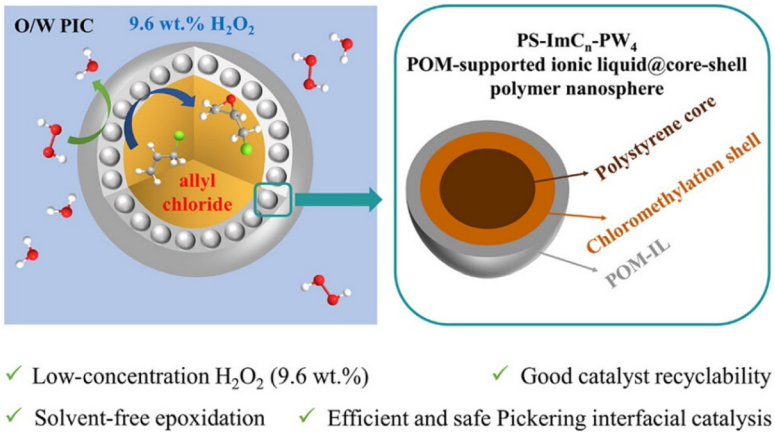

Scheme 4 Epoxidation of allyl chloride with H_2O_2 on PS–ImC$_n$–PW$_4$ catalyst. Adapted from ref. 102 with permission from American Chemical Society, copyright 2023.

catalytic site for the oxidation of alkanes because of the distinctive redox properties of MOCs and the stabilizing effect of ILs.

For example, pairing the task-specifically designed IL-cation of *N*,*N*-bis-2-aminoethyl-4,4-bipyridinium with the Keggin-structured vanadium-substituted POM anion $[PMo_{10}V_2O_{40}]^{5-}$ can result in organic–inorganic hybrid catalyst, which is a catalytically active and recyclable catalyst for cyclohexane oxidation with H_2O_2, giving KA oil (a mixture of cyclohexanol and cyclohexanone).[82] Another example of alkane oxidation using IL–MOCs was reported in Hou's group. Vanadium oxoclusters were synthesized through the condensation of peroxovanadium species in the presence of a functionalized IL [TBA][Pic] (Pic = picolinate ions) with adjustable IL/V molar ratios.[63] The picolinate anion of the IL acted as a ligand to stabilize the oligomeric vanadium oxocluster by coordinating with the vanadium sites, while the cation of the IL played a dual role in charge balancing and fine-tuning the miscibility of the oxocluster in solvents. The molar ratio of IL to V influenced the oligovanadate structure, with the appropriate ratio forming active trimer and dimer configurations. These vanadium oxoclusters exhibited remarkable efficiency as catalysts for the oxidation of cyclohexane, utilizing H_2O_2 as the oxidant. Notably, a significant 30% total yield of KA oil was achieved without the need of additional co-catalysts, and the catalyst demonstrated recyclability due to the incorporation of the IL component. Further studies on the reaction mechanism indicated that the HO$^{\bullet}$ radicals are formed from the adduct of H_2O_2 and vanadium complex, and then the HO$^{\bullet}$ radicals react with alkanes to afford the oxidation products (Fig. 4).

Looking forward, IL–MOC holds promise for alkane oxidation reactions which involve in electron transfer processes, while POMs are well known for their superior redox properties. In the presence of H_2O_2 or molecular O_2, the oxidation of alkanes often proceeds *via* a radical mechanism. POMs could affect reaction kinetics and selectivity by regulating radical pathway of alkane oxidation. Further research to fully understand these mechanisms and optimize POM utilization in alkane oxidation is still underway.

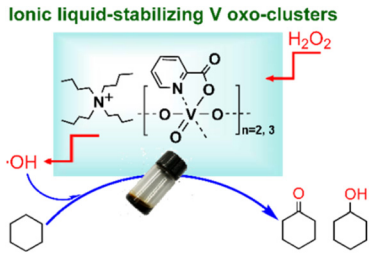

Fig. 4 IL-stabilized vanadium oxo-clusters catalyzing alkane oxidation. Adapted from ref. 63 with permission from Royal Society of Chemistry, copyright 2020.

5.1.4 Alcohol oxidation. Alcohol oxidation is a chemical process involving the conversion of alcohols into carbonyl compounds, aldehydes, or ketones, through the removal of hydrogen. IL–MOCs in alcohol oxidation have emerged as a promising area in catalysis, demonstrating significant advancements in green and sustainable synthetic methodologies.

Early in 2005, the catalytic efficiency of POM–IL $[BMIm]_3[PO_4(W(O)(O_2)_2)_4]$ in alcohol oxidation using IL [BMIm][BF_4] as a solvent was reported.[74] The system exhibited several advantages, including a homogeneous reaction mixture, high product yields, minimal solvent consumption, facile product separation, and the ability to recover and recycle the catalyst without a significant reduction in product yield. Later, Keggin-type $H_3PW_{12}O_{40}$-based di-imidazolium IL hybrids were prepared and exhibited reaction-controlled phase transfer properties with the catalysts precipitated from the aqueous system upon the consumption of H_2O_2 and could be reused several times without loss of activity and selectivity.[71] Similar POM–ILs $[DEDSA]_3[PW_{12}O_{40}]$ and $[DEDSA]_3[PMo_{12}O_{40}]$ (DEDSA = diethyldisulphoammonium) with solvent-responsive

self-separative characteristic were investigated for the oxidation of organic alcohols using hydrogen peroxide as an oxidizing agent.[69] Due to the varied solubility of the hybrids in different solvents, they can effectively catalyze the oxidation reaction in homogenous conditions and then switch back to the heterogeneous system, finally self-precipitate upon the addition of a suitable solvent at the end of the reaction. This special property makes this method an environment-friendly and simpler way for the oxidation of alcohols to aldehydes and ketones. Additionally, $[PW_{12}O_{40}]^{3-}$ immobilized on IL-modified polystyrene resin beads,[90] and into the nanocages of a dual amino-functionalized IL-modified MIL-101(Cr) framework were reported.[91] In the latter case, the dual amino-functionalized IL not only enhances the oxidant accessibility due to the formed hydrogen bonds but also results in increased thermal stability.

V-containing Keggin $H_4PMo_{11}VO_{40}$ was functionalized with ammonium cations with different carbon-chain lengths to form a series of POM-based amphiphilic catalysts.[78] Their catalytic activities were evaluated in the selective oxidation of benzyl alcohol to benzaldehyde using H_2O_2 under organic solvent-free conditions. Among the investigated catalysts, $(ODA)_4PMo_{11}VO_{40}$ (ODA: octadecylmethylammonium) exhibited the highest catalytic efficiency for the selective oxidation with a maximum 61% conversion of benzyl alcohol and a 99% selectivity of benzaldehyde, also offering excellent reusability. Besides, the complexes of decatungstate combined with *N*-butylpyridinium ($[BPy]_4W_{10}O_{32}$) and 1-butyl-3-methylimidazolium ($[BMIm]_4W_{10}O_{32}$) were synthesized in high yields directly from bisulfate-based ILs and used as novel catalysts in the selective oxidation of alcohols to aldehydes or ketones with H_2O_2.[51] Combined with phosphorous cation, the hybrid $(P_{6,6,6,14})_4[W_{10}O_{32}]$ also demonstrated to be a very promising and recyclable catalytic material for alcohol oxidation with acids as the main products under fixed reaction conditions.[52,53]

5.1.5 Selenoether/thioether oxidation. Selenoether oxidation is a chemical process involving the selective oxidation of selenoether groups, which are organic compounds containing selenium atoms bonded to carbon. This reaction converts selenoethers into corresponding sulfoxides or sulfones, it is particularly important for perfluoroalkyl selenoethers, which have oxidized counterparts that are significant but not well-documented in the literature.

POM–IL $(P_{6,6,6,14})_4[W_{10}O_{32}]$ was also proved to be an efficient catalyst for oxidizing perfluoroalkyl selenoethers.[54] A series of perfluoroalkyl selenoxides, selenones, and selenoximines were prepared, with the separation and characterization of enantiomers in some cases. The use of Oxone® as an oxidant allowed the production of perfluoroalkyl selenoxides with electron-withdrawing or donating substituents in different positions (*ortho*, *meta*, or *para*). The reaction also works with various perfluoroalkyl chains and substituents with satisfactory to excellent yields. Overall, the use of POM–IL as a catalyst provides access to the underexplored perfluoroalkyl selenoxides. This study represents the first comprehensive report on the preparation of the perfluorinated selenoximine family with good yields.

Thioether oxidation was achieved by carboxylate IL-stabilized Nb oxoclusters.[58] These clusters, dispersed in polar organic solvents, exhibited "pseudo" liquid phase behavior, enhancing substrate accessibility to catalytic sites. Specifically, [TBA][lactate]-stabilized Nb oxoclusters demonstrated exceptional activity, with TONs more than 56 000 at catalyst loading as low as 0.0033 mol% (1 ppm), which is superior to other Nb-based catalysts. The clusters' flexibility and swelling behavior in polar solvents facilitated substrate access and product diffusion, showcasing their potential as high-performance catalysts for thioether oxidation and beyond.

5.1.6 Biomass oxidation. Biomass oxidation refers to the process of subjecting biomass feedstocks, such as plant materials, agricultural residues, or organic waste, to controlled oxidative reactions. It is a crucial aspect of bioenergy production, providing a renewable and sustainable source of heat, power, and biofuels.

It has been demonstrated that POMs can effectively promote the dissolution of wood in ILs while concurrently reducing the lignin content in the resultant cellulose-rich pulp.[103,104] It's noteworthy that POMs do not completely degrade lignin into low molecular weight fragments, and they can be reoxidized under mild conditions in IL, albeit with some loss in POM and activity. Importantly, different POM species affect significantly the efficiency of delignification. For instance, $[BMIm]_3[PW_{12}O_{40}]$ not only dissolves approximately 30 wt% of cellulosic biomass but also converts biomass into commodity monosaccharides like glucose and xylose.[105] Some examples of biomass oxidation using IL–MOCs as catalysts are shown in Table 3.

Since lignin is resistant to conversion due to its complex structure and stable linkages, acid-catalyzed lignin degradation to phenolic monomers has gained great interest due to its potential for producing biofuels and chemicals.[112] Back in 2016, Welton *et al.* used acidic $H_5PV_2Mo_{10}O_{40}$ as a catalyst coupled with protic IL $[HC_4Im][HSO_4]$ as the solvent, together with molecular oxygen and hydrogen peroxide to depolymerize lignin samples extracted from pine and willow.[106] Besides phenols and functionalized aromatics, vanillin and syringaldehyde were the main products extracted from the IL. This system succeeds in the synergistic properties of ILs to depolymerize lignin and the remarkable properties of the POM to oxidize the lignin fragments into useful platform chemicals. Exchanging the protons with imidazolium cations produced $[HC_4Im]_5PV_2Mo_{10}O_{40}$ and $[HC_2Im]_5PV_2Mo_{10}O_{40}$ hybrids, which also showed high efficiency in the oxidation of lignin fragments into platform compounds in aqueous acidic ILs solutions.[80] Lignin conversion could reach to 76% with 77% selectivity of ketone products (acetovanillone, 3-methoxyphenol, and 4-methylcatechol). With $[HC_4Im]_3PMo_{12}O_{40}$ as a catalyst produced phenolic products (mainly *m*(*p*)-cresol, veratrole, vanillin). It was found the POM–IL type and the IL acidity had a big influence on the reaction process. The lignin molecule not only had intermolecular hydrogen bonds and π–π stacking with the imidazole ring, but also formed stronger hydrogen bonds with POM anions, thus making the lignin structure

Table 3 Some examples of biomass oxidation using IL–MOCs as catalysts

IL–MOCs	Solvent	Starting material	Products	Ref.
$[EMIm]_4H[PV_2Mo_{10}O_{40}]$	[EMIm]OAc	Lignocellulosic biomass	Cellulose-rich pulp	103
$[BMIm]_3[PW_{12}O_{40}]$	None	Biomass	Monosaccharides such as glucose and xylose	105
$H_5PV_2Mo_{10}O_{40}$	$[HC_4Im][HSO_4]$	Lignin samples extracted from pine and willow	Vanillin and syringaldehyde	106
$[HC_4Im]_3PMo_{12}O_{40}$, $[HC_4Im]_5PV_2Mo_{10}O_{40}$, $[HC_2Im]_5PV_2Mo_{10}O_{40}$, $[HC_4Im]_4SiMo_{12}O_{40}$	Acidic IL	Alkali lignin	Various aromatic compounds	80
HPMoV–C_4C_1Im–SO_3H	DMSO	2-Phenoxy-1-phenylethanol	Benzoic acid and phenol	107
$[C_2COOHC_1IM]_4H[PV_2Mo_{10}O_{40}]$	Deionized water	Carbohydrates	Glycolic acid	108
$BetH_5V_2Mo_{18}$	None	Native lignocellulose of pinewood and poplar wood	Ethyl vanillate, ethyl syringate, vanillin, and syringaldehyde	109
[BIm][Pic]-stabilized V_2O_5	MeOH	β-O-4 lignin model compounds	Phenols, eaters, and acids	64
$[BSmIm]CuPW_{12}O_{40}$	Ethanol–water mixture	Wheat stalk lignin	Diethyl maleate	110
$[BSmIm]CuPW_{12}O_{40}$	Ethanol	Raw lignocellulosic biomass	Diethyl maleate	111
$[PyBS]_5PV_2Mo_{10}O_{40}$	H_2O	Cellobiose/cellulose	Formic acid and levulinic acid	81
$[MIMPS]_3HPMo_{11}VO_{40}$, $[PyPS]_3HPMo_{11}VO_{40}$, $[TEAPS]_3HPMo_{11}VO_{40}$, $[BMIm]_3HPMo_{11}VO_{40}$	H_2O	Cellulose	Formic acid	79

more flexible and easier to depolymerize. Later, a series of POM–ILs were reported for the selective cleavage of the β-O-4 linkage to value-added aromatic chemicals under mild conditions. Lv and Yang *et al.* reacted $H_5PV_2Mo_{10}O_{40}$ with 1-methyl-3-(4-sulfobutyl)-1*H*-imidazolium (C_4C_1Im–SO_3) zwitterions to form the HPMoV–C_4C_1Im–SO_3H POM–IL assembly,[107] which could also selectively and effectively convert various β-O-4 lignin models into aromatic acids and phenols under mild homogeneous conditions. It could be precipitated by the addition of ethyl acetate to the homogeneous post-reaction solution, thus could be reused for five runs. Similarly, IL $[C_2OHC_1Im]Br$ (1-(hydroxyethyl)-3-methylimidazole bromide) was assembled with $H_5PV_nMo_{12-n}O_{40}$ (n = 1–3) to form POM–ILs with different V molar ratios.[108] Among them, $[C_2COOHC_1Im]_4PVMo_{11}O_{40}$ could oxidize glucose and its upstream biomass derivatives to glycolic acid under O_2 with 88% conversion and 61% selectivity, which is even applicable to the oxidation of raw lignocellulose.

Deep eutectic solvent cation betaine was combined with Dawson-type $H_6V_2Mo_{18}O_{62}$ to form $BetH_5V_2Mo_{18}O_{62}$ material, and it could be used as a trinitarian catalyst for one-pot lignocellulose transformation.[109] The incorporation of Bet^+ cation with POM anion not only increases the activity due to the strong hydrogen bonding interactions between the Bet^+ cation and substrate 2-phenoxy-1-phenylethanol but also forms a micro-environment that concentrates solid lignocellulose to overcome mass-transferring barriers. Furthermore, the Bet^+ endowed $H_6V_2Mo_{18}O_{62}$ with temperature responsibility, ensuring the recyclability of $BetH_5V_2Mo_{18}O_{62}$.

Besides acidic HPMoV, neutral vanadium pentoxide stabilized by IL is also efficient for biomass oxidation. Hou *et al.* used imidazolium IL [BIm][Pic] to stabilize the vanadium oxocluster catalysts, and the catalyst showed superior activity for one-step selective oxidation to cleave the β-O-4 linkage of lignin model compounds to phenols, eaters, and acids.[64] It was found the presence of mixed-valence state of V^{4+} and V^{5+} in V oxocluster catalysts was crucial for enhancing the catalytic activity, and the oligomeric states of V species could be tuned by adjusting the molar ratio of IL [Bim][Pic] to V. Especially, 1-butylimidazolium also played a facilitating role in the cleavage of C–O bonds by the action of the protonated IL cations. Notably, the catalyst can be recycled with the catalytic activity did not decrease significantly even after five cycles (Fig. 5). This catalytic system demonstrates a new approach for the selective aerobic oxidation of β-O-4 lignin without any co-catalysts.

Meanwhile, POM–IL $[BSmIm]CuPW_{12}O_{40}$ catalytic systems have been developed for the production of diethyl maleate in Li's group.[110,111] Under optimized conditions, 94% wheat stalk lignin was oxidized with 73% diethyl maleate selectivity over $[BSmIm]CuPW_{12}O_{40}$ *via* oxidative ring cleavage of lignin, followed by *in situ* esterification in one pot.[110] A series of phenol, guaiacol, syringol, and their derivatives could be oxidatively converted into diethylmaleate. Later, to broaden the substrate scope, a one-step selective conversion of raw lignocellulosic biomass directly to diethyl maleate over the [BSmIm]

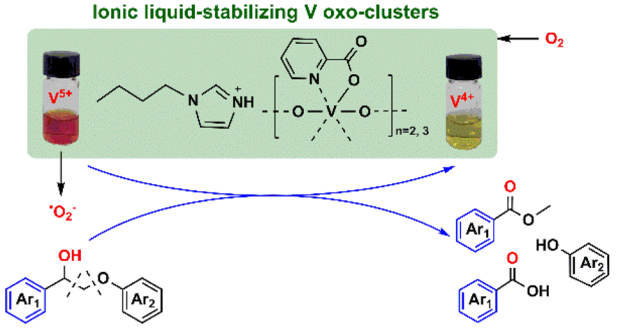

Fig. 5 IL-stabilized vanadium oxocluster catalysts for selective oxidative cleavage of β-O-4 lignin model compounds. Adapted from ref. 64 with permission from American Chemical Society, copyright 2023.

$CuPW_{12}O_{40}$ catalyst was proposed.[111] All major fractions of lignocellulose could be converted simultaneously into diethyl maleate with high selectivity. It was found that the relatively low incorporation of the Cu^{2+} sites in $[BSmIm]CuPW_{12}O_{40}$ (in comparison with that of $CuHPW_{12}O_{40}$) gives vacant orbitals for molecular oxygen, which is responsible for the excellent catalytic activity. Additionally, the $[BSmim]CuPW_{12}O_{40}$ could be easily recovered from the mixture after the reaction by simple temperature control.

One-pot transformation of cellulose directly into formic acid (FA) and levulinic acid (LA) is possible *via* vanadium-containing POM–IL catalysts.[113] A relatively high selectivity of LA (46.3%) and FA (26.1%) together with 100% cellobiose conversion could be obtained by using $[PyBS]_5PV_2Mo_{10}O_{40}$ as a catalyst.[81] It could be easily recycled four times without a significant loss of activity. Meanwhile, a similar POM–IL $[MIMPS]_3HPVMo_{11}O_{40}$ was applied in the conversion of cellulose into FA with over 50% FA yield and a high FA concentration of ~10% in aqueous solution.[79] Notably, these POM–ILs acted as bifunctional catalysts, with $-SO_3H$ functionalized cations catalyzing cellulose hydrolysis to glucose and POM anions catalyzing glucose oxidation to FA.

Overall, acidic IL–MOC materials are efficient for biomass oxidation, representing an innovative approach with significant implications for sustainable energy and chemical production. The synergistic effect between the IL cation and MOC anion facilitates the controlled oxidation of biomass components, such as lignocellulosic materials, under mild conditions to value-added products without any additives.

5.1.7 Oxidative desulfurization. Oxidative desulfurization (ODS) is a chemical process aimed at removing sulfur compounds from fuels like diesel and gasoline. Compared with traditional hydrodesulfurization, ODS is highly effective, functioning much better under mild reaction conditions, and has become an attractive research topic in recent years.[114] Commonly used oxidizing agents in ODS include hydrogen peroxide and various peroxy acids. Keggin and Dawson-type HPAs have been intensively studied because of their discrete ionic structure and high proton mobility.[115] However, HPAs have shortcomings such as high solubility in polar solvents, low specific surface area, and acidic catalyst properties that may cause equipment corrosion. The usage of POM–ILs successfully overcomes these problems with substantially increased catalytic activity and reusability. ILs serve not only as phase transfer catalysts but also as the solvents for the reaction to take place and extractants of the oxidized sulfur compounds. Organic cations, including quaternary ammonium, imidazolium, and pyridinium, have high affinity with aromatic sulfur compounds and thus showed phase transfer ability, especially for the aromatic cations. This ability is assumed to be influenced by π–π interaction, determined by the electron density on the aromatic ring.

Recently, Hou's group developed novel carboxylic acid-functionalized imidazolium IL-stabilized Ti oxoclusters.[65] These oxoclusters, well stabilized in ILs and highly dispersed in methanol, showed excellent desulfurization efficiency under mild conditions. Complete removal of sulfur compounds from model oil was achieved using the Ti oxo-HSO_4 catalyst, with methanol identified as the most effective extractant. It was indicated that Ti–OOH species were indeed the active species and responsible for the sulfur removal on the Ti oxocluster catalysts. Moreover, the HSO_4^- anion could activate the Ti–OOH species by forming hydrogen bonds, facilitating the electrophilic oxygen transfer in the ODS reaction. This strategy provides an alternative and green route for constructing stable MOC catalytic systems (Scheme 5).

Several review papers focusing on ODS reactions using POM–ILs as catalysts have been published, including works by Yu *et al.*,[116] Zhao *et al.*,[117] Ong *et al.*,[118] and Anbia *et al.*[119] Specifically, the reported examples until March 2021 are detailedly summarized by Anbia *et al.*[119] Beyond the commonly studied tungstenphosphoric or phosphomolybdenum-based POM–(P)ILs,[120,121] tungstovanadate-based POM–IL $[C_2(MIm)_2]_2VW_{12}O_{40}$ (MIm = 1-methylimidazolium) was also

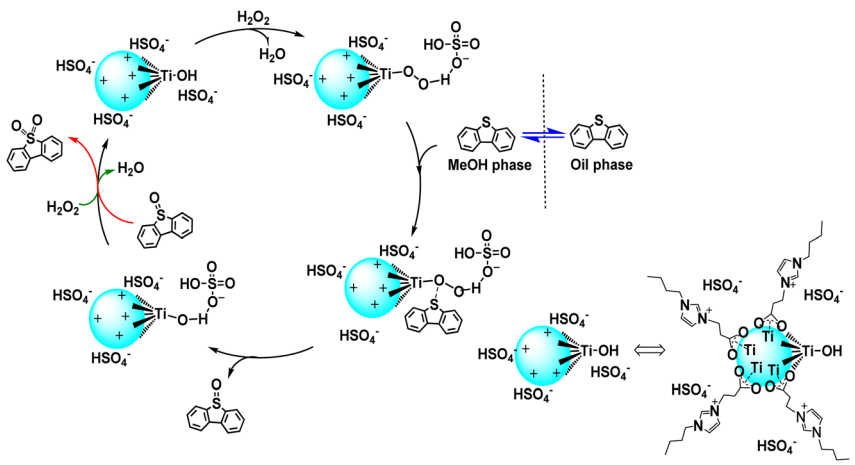

Scheme 5 Proposed mechanism for the extraction and catalytic oxidative desulfurization (ECODS) system catalyzed by Ti oxocluster catalyst. Adapted from ref. 65 with permission from American Chemical Society, copyright 2022.

investigated as a catalyst in ODS with 100% sulfur removal efficiency and sulfone product selectivity in 20 min, with a high turnover frequency (TOF) value (53.2 h^{-1}).[122]

In addition, the heterogeneous carboxyl-functionalized bilayer POM–IL catalysts were also developed, demonstrating superior activity for ODS (Scheme 6).[123] The optimized catalyst, SiO_2 (50 nm)–BiIL–PW (Keggin-type), exhibits good amphiphilicity for both sulphur-containing compounds and hydrogen peroxide, thereby providing a quasi-homogeneous microenvironment for the heterogeneous catalysis. Complete sulfur removal can all be achieved for four model fuels free of extractant. It was demonstrated that POM and carrier have significant effects on the catalytic activities. Notably, no decrease in catalytic efficiency was observed even after the eight cycles in scale-up experiments. These results make the catalyst promising for industrial application.

Besides, SiO_2, graphene oxide (GO) was also used as a supported material for POM–IL in ODS reactions.[124,125] One example involves the synthesis of POM–ILs with monomer, dimer, and poly IL, and then further loaded on the surface of GO.[124] The influences of IL type and carrier on ODS activity were thoroughly investigated. The other example is the covalent immobilization of POM–IL on the amine-modified magnetic GO (APTES-mGO).[125] The employed ILs were imidazolium cation-based, with varying alkyl chain lengths (C_n[MIm]Cl, n = 4, 8, 12, and 16). Among these, $[C_{12}MIm]_5PV_2Mo_{10}$/APTES-mGO, with a C_{12} alkyl length chain, showed the highest sulfur removal percentage due to its desirable amphiphilicity, which facilitated a stable Pickering emulsion system, enhancing the contact area between phases and overcoming mass transfer resistance. The emulsion breakage and the catalyst recycling can be achieved using a permanent magnet. Notably, the designed catalyst could be recovered 8 times without significant loss of its catalytic activity.

5.1.8 Hydroxylation of benzene. Hydroxylation of benzene refers to the chemical process of introducing a hydroxyl (–OH) group onto a benzene ring *via* selective oxidation. For the IL–MOC catalysts, V-containing Keggin-type heteropolyanion combined with various IL cations are the most widely studied, mainly with molecular oxygen or H_2O_2 as the oxidant. For example, a series of $PMo_{10}V_2O_{40}^{5-}$ anion-based POM–ILs have been constructed in Wang's group and employed for hydroxylation of benzene.[126–132] Additionally, a nitrogen-doped biomass carbon catalyst SFNC(800) was developed through direct carbonization of soybean flour at 800 °C.[133] By combining the SFNC(800) with the Keggin-type V-POM, a recyclable catalytic system with molecular oxygen as the oxidant towards liquid-phase reductant-free aerobic oxidation of benzene to phenol was built. The resulting hybrid catalyst exhibits an interesting temperature-controlled phase-transfer feature, facilitating easy catalyst recycling.

Phosphovanadomolybdate (V-POM) in other compositions ($H_7[P_2Mo_{17}VO_{62}]$, $H_8[P_2Mo_{16}V_2O_{62}]$ and $H_9[P_2Mo_{15}V_3O_{62}]$) were combined with amphiphilic PIL (Scheme 7).[21] These composites served as efficient heterogeneous catalysts for the direct hydroxylation of benzene to phenol with H_2O_2 in the liquid phase. The synergistic catalytic effect between the V-POM anion and carboxylic acid-functionalized PIL cation framework contributed to the high catalytic performance. Meanwhile, $H_2PMo_{11}VO_{40}^{2-}$ anion-based imidazolium IL was also employed as a catalyst for the hydroxylation of benzene by H_2O_2 without using a solvent.[134] The homogeneous emulsion formed by the catalyst and substrates during the reaction facilitated the catalytic process. After the reaction, the catalyst could self-precipitate from the reaction media and proved to be recyclable. Moreover, mesoporous MCM-41[135] and functionalized chloromethylated polystyrene[136] were employed as supported materials for V-POMs to enhance the recyclability of the active species.

In addition to V-POMs, vanadium oxocluster itself is also effective for hydroxylation of benzene. For example, V_xO_y supported on PIL (V_xO_y/PIL) demonstrated much higher catalytic performance than the analogous catalyst V_xO_y/P, prepared with only the polymer support (P), without the IL. The superior catalyst performance of V_xO_y/PIL might be assigned to a higher specific surface area, stronger absorbent ability, and more active sites than the smooth and bulky V_xO_y/P.[137] Furthermore, the hydrophobic side chain of the IL in the catalyst was beneficial for the access of benzene and the removal of the generated phenol from the surface of the catalyst, which also played an important role in improving the catalytic performance. In addition, the catalyst is highly stable and recycled at least three times without a significant decline in the phenol yield.

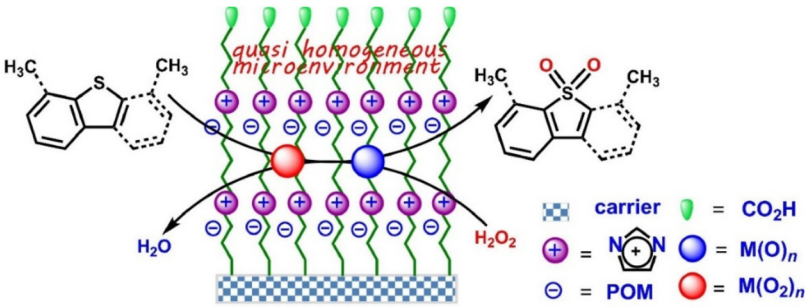

Scheme 6 The diagram of ODS catalyzed by SiO_2–BiIL–CO_2H–POM. Adapted from ref. 123 with permission from Elsevier, copyright 2023.

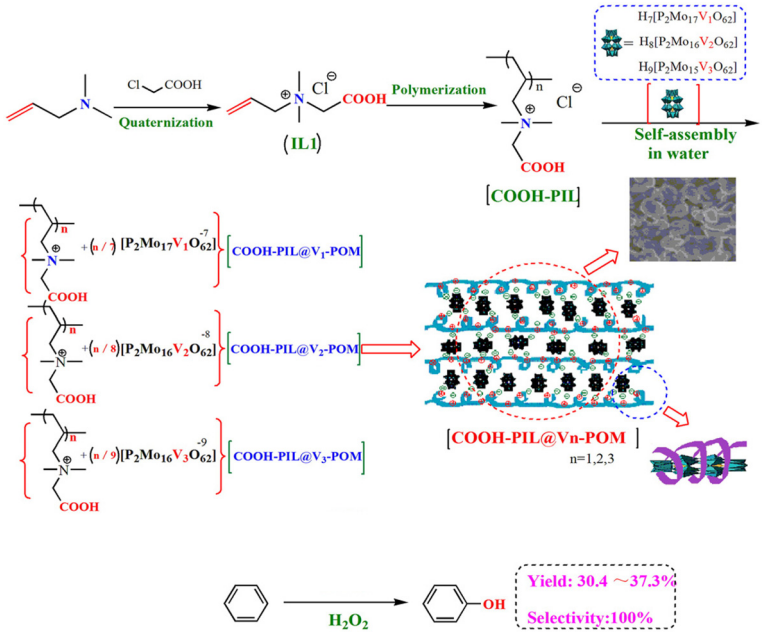

Scheme 7 Direct hydroxylation of benzene to phenol with H_2O_2 catalyzed by three porous functionalized PIL/phosphovanadomolybdate ionic composites. Adapted from ref. 21 with permission from Wiley-VCH Verlag GmbH, Weinheim, copyright 2020.

5.2 The acid catalysis

5.2.1 Esterification. The esterification reaction is the condensation of a carboxylic acid with an alcohol, resulting in the formation of an ester and water. Catalyzed by acids or bases, esterification is a versatile tool in the synthesis of a wide range of compounds, including biodiesel production. The first catalytic application of POM–IL salts for esterification reaction, with one of the reactants being polycarboxylic acid or polyol, was reported by Wang *et al.* early in 2009.[66] The salts ($[MIMPS]_3PW_{12}O_{40}$, $[PyPS]_3PW_{12}O_{40}$, and $[TEAPS]_3PW_{12}O_{40}$) are considered as "reaction-induced self-separation catalysts". Their solubility in polycarboxylic acids or polyols, nonmiscibility with ester products, and high melting points facilitate the switch from homogeneous to heterogeneous catalysis after the completion of the reaction, enabling convenient recovery and reuse of the POM–IL catalysts. Additionally, a new family of poly(ethylene glycol)-functionalized alkylimidazolium, paired with Keggin-type HPA, has proven effective in the esterification of alcohols with acetic acid as well with self-separation property.[66] An emulsion forms between the IL catalyst and substrates during the reaction, promoting the catalytic process. After the reaction, the emulsion can be conveniently broken by the addition of a weakly polar organic solvent to facilitate the catalyst separation. Inspired by these results, a direct transformation of benzaldehyde to methyl ester under relatively mild conditions has been developed in the absence of any cocatalyst.

Meanwhile, POM–IL immobilized on MOF was prepared and applied for the esterification of acidic vegetable oil.[95] MOFs (UiO-66-2COOH) were functionalized with Keggin-type POM acids first and then further incorporated with sulfonated acidic ILs. The resulting ILs/POM/UiO-66-2COOH solid catalyst combines Brønsted and Lewis acid sites, exhibiting a high surface area, increased acidity, and exceptional catalytic activities with long-term stability and reusability for one-pot biodiesel production *via* esterification of the low-cost acidic oils. Therefore, this solid catalyst has potential for practical application in the catalytic biodiesel production, and would provide a guide for selecting suitable POM–ILs for the preparation of solid acid catalysts.

5.2.2 Acetalization. Acetalization is the organic reaction that converts carbonyl compounds, such as aldehydes and ketones, into acetal (or ketals) through the reaction with alcohols in the presence of an acid catalyst. One example of the usage of POM–IL in acetalization was reported by Han and Liu *et al.*[75] Transition-metal (M = Mn, Fe, Co, Ni, Cu) ion-exchanged $H_3PW_{12}O_{40}$-based IL catalysts were synthesized by mixing $H_3PW_{12}O_{40}$ with metal precursors and methylimidazolium propyl sulfobetaine (MIMPS) zwitterionic IL precursors, and they were then exploited for the acetalization of benzaldehyde with ethylene glycol. These formed organic–inorganic, water-soluble composite salts not only possess strong Brønsted and Lewis acidities but also exhibit unique self-separation properties desirable for catalyst separation and recycling. Among them, the $Ni[MIMPSH]PW_{12}O_{40}$ catalyst showed extraordinary catalytic performance and durability, achieving a benzaldehyde glycol acetal with 99% selectivity and 95% yield. Further kinetic studies revealed an activation energy of 34 kJ mol^{-1} for the acetalization reaction, surpassing most reported catalysts.

5.2.3 Transesterification. Transesterification is the conversion of a carboxylic acid ester into a different carboxylic acid

ester. The most common method involves the reaction of the ester with an alcohol in the presence of an acid or base catalyst. Strong acids catalyze the reaction by donating a proton to the carbonyl group, thus making it more electrophilic, while bases catalyze the reaction by removing a proton from the alcohol, thus making it more nucleophilic. Three examples are presented in Table 4.

Polyethylene terephthalate (PET) is widely used in daily life, particularly in food packaging. To decrease environmental pollution and resource wastage issues, PET degradation is of great significance. Compared with the physical and hydrolysis methods, PET alcoholysis is a more favored degradation approach. Lu *et al.* found that transition-metal-substituted POMs $Na_{12}[WZnM_2(H_2O)_2(ZnW_9O_{34})_2]$ (M = Zn^{2+}, Mn^{2+}, Co^{2+}, Cu^{2+}, Ni^{2+}) can efficiently catalyze PET alcoholysis,[138] with superior activity than transition single-substituted catalyst $K_6SiW_{11}ZnO_{39}(H_2O)$ due to their specific sandwich structure, increased active sites, and outstanding coordination ability with PET carbonyl oxygen. Then they synthesized a series of POM–ILs with different anion–cation molar ratios to investigate the possible impact of the layer spacing of the catalyst on PET degradation since polymer degradation simultaneously requires the active site of the catalyst to match multiple reaction sites in the polymer long chain (Scheme 8).[139] It was found that the adjustable layer spacing (1.00–1.63 nm) in these POM–ILs, achieved by incorporating $[WZn_3(H_2O)_2(ZnW_9O_{34})_2]_{12}$ anion with organic cations such as pyridinium (Py), 3-(pyridine-1-ium-1-yl)propane-1-sulfonate (PyPs), 1-(3-sulfonic group) trimethylamine (TEAPs), and 1-methyl-3-(3-sulfopropyl)imidazolium (MIMPs), was a crucial parameter. When the catalyst layer spacing was adjusted to coincide with the spacing of 1.32 nm between the carbonyl active sites on both sides of the PET benzene ring, the active sites of the catalyst (Zn atom in the POM and N atom in the pyridine ring) corresponded exactly to the reactive sites in PET's long chain. This enabled the shearing of the carbonyl functional group at a fixed point on the nanoscale, promoting fast and complete reaction. Thus the transformation of POM into POM–IL not only enhances thermal stability but also introduces anionic and cationic synergistic catalysis. Under optimal conditions, the proposed catalytic strategy achieved complete PET degradation in just 30 minutes, with a remarkable 85% yield of bis(hydroxyethyl) terephthalate (BHET). Impressively, the BHET yield remained consistently above 85% even after five cycles, highlighting the sustainability and robustness of the approach. This innovative strategy of precisely modulating the spacing of the catalytic active site represents a significant advancement in the field of PET alcoholysis, which also provides a new approach for designing functional catalytic materials tailored for depolymerizing waste plastics into high value-added chemicals.

Furthermore, titanium-centered POM–ILs, denoted as $[BMIm]_{4-6}[M(H_2O)TiMo_{11}O_{39}]$ (M = Cu^{2+}, Fe^{2+}, Pb^{2+}, Ti^{4+}, and Zn^{2+}), were evaluated in the alcoholysis of bottle-grade PET, using waste mineral water bottles as samples.[83] Among the catalysts, $[BMIm]_4[Ti(H_2O)TiMo_{11}O_{39}]$ exhibited optimal catalytic efficacy, achieving a 100% alcoholysis rate and a 85% BHET yield with a catalyst dosage of 0.6% at 190 °C for 5 hours. Impressively, even after six cycles, the alcoholysis rate remained as high as 94% with 76% BHET yield. These findings highlight the potential of the prepared POM–IL catalysts in catalyzing the degradation of bottle-grade PET, offering a promising avenue for sustainable waste management. Meanwhile, this POM–IL $[BMIm]_4[Ti(H_2O)TiMo_{11}O_{39}]$ behaved as a phase transfer catalyst for the transesterification reaction between dimethyl carbonate and phenol to synthesize diphenyl carbonate.[84] Under optimized conditions, the phenol conversion reached 46%, and the overall selectivity of mono- and diphenyl carbonate products was 99%. Moreover, the catalyst could be reused four to five times due to its characteristic of a "homogeneous phase at high temperature and separation at low temperature".

5.3 The CO_2 activation and utilization

The utilization of CO_2, a greenhouse gas and also a valuable C1 feedstock, reduces reliance on traditional fossil fuel-based resources, fosters more sustainable pathways, and contributes to the concept of a circular economy by closing the carbon loop.

The POM–IL catalytic systems demonstrate the ability to activate CO_2 through cooperative interactions between the POM and IL components. The POM acts as a redox-active entity, facilitating electron transfer during the activation of CO_2, while the IL provides a stabilizing medium for the POM and influences the solubility and reactivity of CO_2. The catalytic transformations of CO_2 using POM–IL catalytic systems have been summarized previously,[140,141] which demonstrates the advantages of POM-based ILs in the emerging field of CO_2 utilization, *e.g.* CO_2 capture, the cycloaddition of CO_2 to epoxides, and reduction of CO_2. Here, we mainly focus on new cata-

Table 4 Examples of transesterification in the catalytic degradation of polyethylene terephthalate

	Amount/g								
Catalysts	Cat.	Sub.	Sol.	*T*/°C	*t*	Conv./%	Yield/%	Reuse cycles	Ref.
$Na_{12}[WZn_3(H_2O)_2(ZnW_9O_{34})_2]$	0.025	5.0	20.0	190	40 min	100	84	Four	138
$[PyPs]_6[WZn_3(H_2O)_2(ZnW_9O_{34})_2]$	0.04	5.0	20.0	195	0.5 h	100	85	Five	139
$[BMIm]_4[Ti(H_2O)TiMo_{11}O_{39}]$	0.21	5.0	30.0	190	5 h	100	85	Six	83

Substrate: polyethylene terephthalate (PET), product: bis(hydroxyethyl) terephthalate (BHET), solvent: ethylene glycol.

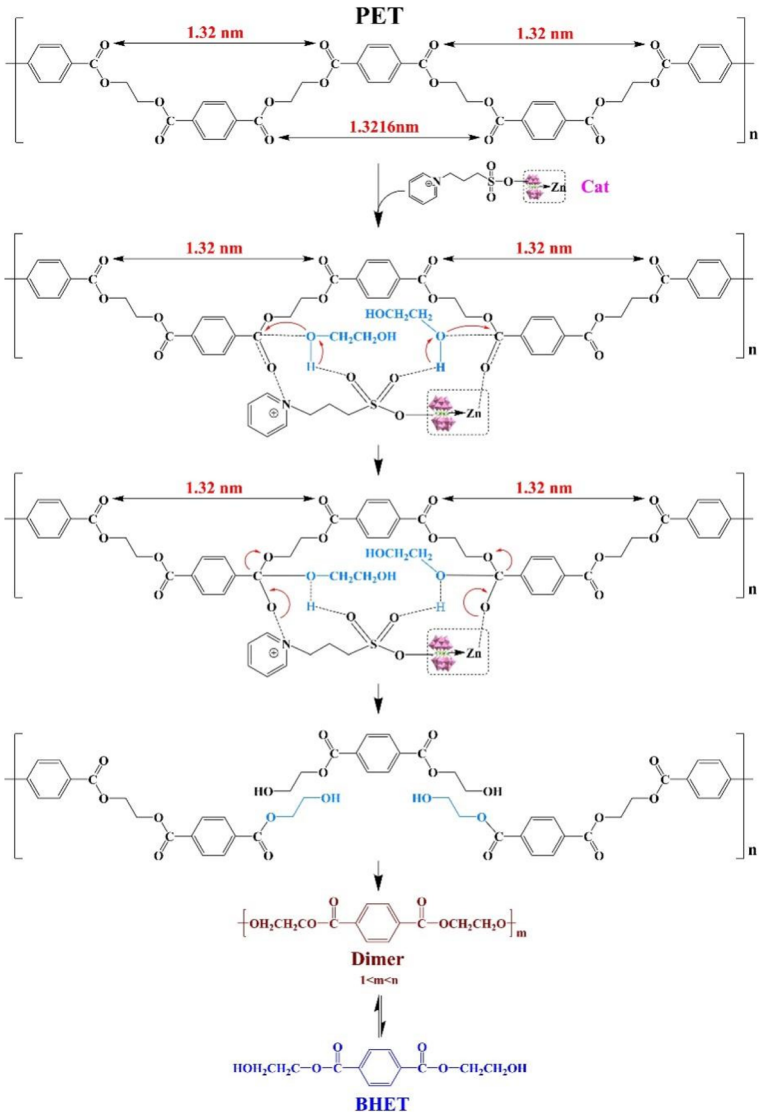

Scheme 8 The schematic illustration of the possible mechanism of PET alcoholysis with POM–IL. Adapted from ref. 139 with permission from Wiley-VCH Verlag GmbH, Weinheim, copyright 2023.

lytic designing and new catalytic effects in CO_2 utilization by POM–IL catalytic systems in recent three years.

5.4 The catalytic carbonylation

Carbonylation refers to reactions that introduce carbon monoxide into organic and inorganic substrates. Carbonylations form the basis of many types of reactions, *e.g.* hydroformylation, hydrocarboxylation/hydroesterification, aminocarbonylation, and *N*-formylation of CO_2, *etc.*

Catalytic hydroformylation is a pivotal industrial process in which alkenes react with carbon monoxide and hydrogen, typically in the presence of a transition metal catalyst like rhodium, to yield aldehydes. The POM–IL–Rh SAC $(MTOA)_5[SiW_{11}O_{39}Rh]$ (MOTA = methyltrioctylammonium cation) is active for the hydroformylation of alkenes to produce aldehydes at an ultralow loading of Rh (*ca.* 3 ppm) (Fig. 6), displaying exceptional catalytic activity and long storage stability.[100] For styrene hydroformylation, both the conversion and the aldehyde yield can reach almost 99%, and a TOF as high as 9000 h^{-1} was obtained without using any phosphine ligand. This IL catalyst, miscible with *n*-hexane at reaction temperatures, contributed to the exceptionally high activity, while the bulk organic cation not only prevented active Rh species from leaching during reactions but also stabilized Rh^1 species from reducing into Rh^0 species.

Catalytic hydrocarboxylation is a transformative process wherein alkynes or alkenes undergo carboxylation in the presence of carbon monoxide and water, typically facilitated by transition metal catalysts like nickel or palladium. The Keggin-type POM–IL–Pd SACs $[(n\text{-}C_4H_9)_4N]_6[SiW_{11}O_{39}Pd]$ and $[(n\text{-}C_4H_9)_4N]_5[PW_{11}O_{39}Pd]$, with Pd atoms incorporated into the POM structure, exhibited high efficiency in the olefin hydrocar-

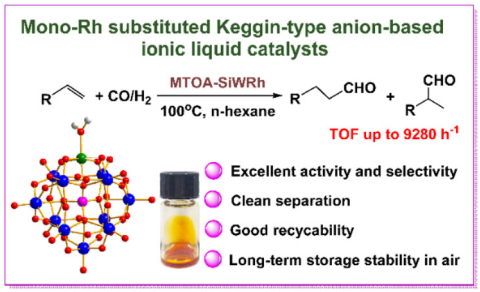

Fig. 6 Ionic liquid-immobilized rhodium single-atom catalyst for hydroformylation. For the ball-and-stick structure of the $[SiW_{11}O_{39}Rh(H_2O)]^{5-}$ framework: Si, W, O, Rh and H atoms are shown in pink, blue, red, green and gray spheres, respectively (inset). Adapted from ref. 100 with permission from Wiley-VCH Verlag GmbH, Weinheim, copyright 2022.

boxylation reaction under two-phase conditions, achieving up to 95% conversion of styrene and 95% carboxylic acid yield at 110 °C.[88] The tetrabutylammonium cation played a crucial role in stabilizing the Pd catalyst, allowing for easy storage and consecutive catalytic recycling. Mechanistic studies revealed a reaction pathway proceeding through the "Pd–H" pathway, with the Pd SAC system exhibiting superior performance and stability even without phosphine ligands. This catalytic system offers advantages such as broad substrate suitability and easy quantitative recovery, with ongoing efforts to further enhance its efficiency.

The catalytic *N*-formylation of CO_2 involves the incorporation of CO_2 into organic substrates to form *N*-formyl compounds. The POM–IL–Ru SAC ($[TOMA_6SiW_{11}O_{39}Ru(dmso)]$, TOMA = methyltrioctylammonium) with the single-atom Ru, confirmed to be anchored into the framework of the POM, demonstrated high efficiency in the *N*-formylation of amines with CO_2 and H_2 in toluene-IL biphasic media (Fig. 7).[89] The binary IL system, involving the POM-based IL and [BMIm]OAc, exhibited a sponge-like structure, ensuring efficient contact between catalytic sites and substrates. Experimental results and the DFT calculations indicated a pathway that involves formate intermediates, and the process is a three-component (morpholine, Ru–POM–IL, and BMImOAc) synergistic process,

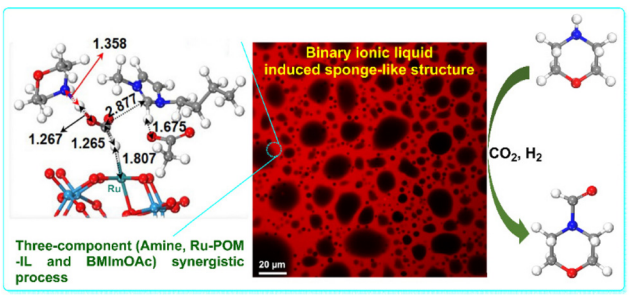

Fig. 7 Ruthenium single-atom anchored in POM–ILs for *N*-formylation of amines with CO_2 and H_2. Adapted from ref. 89 with permission from American Chemical Society, copyright 2023.

which significantly reduces the reaction energy barrier and enhances the conversion and yield, showcasing the catalytic system's advantages in terms of high efficiency, robustness, and recyclability in *N*-formylation reactions.

Additionally, Hou's group developed new-type organic ammonium cation-stabilized Nb oxoclusters, which can efficiently catalyze the reductive amination of CO_2 with amines using $PhSiH_3$ as a reducing agent.[142] The reaction proceeds smoothly under ambient conditions and affords formamides with excellent selectivity. Notably, the Nb oxocluster catalysts showed good recyclability in consecutive recycles and wide substrate suitability. Mechanistic studies suggest that the *N*-formylation reaction proceeds *via* a silyl formate reaction path. The organic methyltrioctylammonium cation could not only prevent Nb oxoclusters from aggregation, but also provide the suitable hydrophobic environment to accelerate the accessibility of organic reactants to the catalytic active centers. As a result, the POM–IL catalyzed CO_2 activation showcases the potential for developing sustainable and environmentally friendly processes for utilizing CO_2 as a carbon source, contributing to the field of green chemistry and carbon capture and utilization.

5.5 Catalytic hydrogenation/hydrogenolysis

Catalytic hydrogenation and hydrogenolysis are chemical processes used to modify or transform organic compounds by introducing hydrogen atoms into the molecular structure. POMs doped with Pd,[143] Pt[144–147] and Ru[148,149] nanoparticles (NPs) are reported to be efficient hydrogenation/hydrogenolysis catalysts. Han *et al.* designed a multifunctional catalyst denoted as Pd NP/POM–IL composite supported on SiO_2 (Pd/H_2[POM–IL]@SiO_2) for the reductive hydrolysis of C–O bonds in diaryl ethers in water, yielding selective ketone products in high yields (>80%) (Fig. 8).[150] The alcohol byproducts, which are common products from this kind of reaction, and compli-

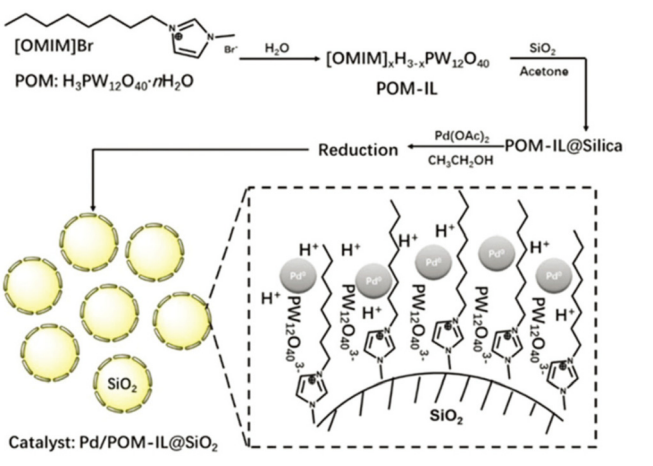

Fig. 8 Schematic illustration of the process for the synthesis of multifunctional catalyst Pd/POM–IL@SiO_2 (Pd/H_x[OMIM]$_{3-x}PW_{12}O_{40}$@SiO_2, x = 1, 2, 3) and its structure. Adapted from ref. 150 with permission from Royal Society of Chemistry, copyright 2018.

cate product purification are deliberately excluded. The catalytic reaction cannot proceed in the absence of either a catalyst or H_2 (in 3 MPa N_2). Without the incorporation of Pd NPs, the POM–IL@SiO_2 alone could not catalyze the reaction either. So the unique performance of the catalyst results from the excellent cooperation of Pd NPs, POM, and imidazolium cation, with Pd and POM co-catalyze the reaction and imidazolium cation enhances the accumulation of the reactants due to its hydrophobic nature. The catalyst exhibited efficacy not only for diaryl ethers but also for alkyl aryl ethers, facilitating their transformation into the corresponding ketones. Notably, the catalyst demonstrated robustness and stability throughout the reaction even after five successive reuses. This study introduces a promising avenue for the valorization of lignin derivatives, including authentic lignin from raw biomass, into valuable chemical products in a sustainable, efficient, and highly selective manner.

In quinoline hydrogenation, our recent investigation demonstrates that the POM anion-stabilizing Pt nanocatalysts can greatly facilitate to forming oxygen vacancies adjacent to Pt^0 species on POM catalysts.[147] The oxygen vacancy concentration of the POM catalyst exhibited a decisive role in the catalytic hydrogenation of quinoline in the aqueous media. Further studies indicated H_2O actually participated in the hydrogenation and acted as an indirect hydrogen source. Especially, H_2O was adsorbed at oxygen vacancies and underwent homolytic cleavage into OH^- and H^- species, and the forming interfacial platinum–hydroxyl species can efficiently promote the heterolytic H_2 dissociation for hydrogenation. It was noteworthy that organic cations exert a remarkable impact on oxygen vacancy density, which implies that the catalytic performance enables it to be tuned by the cation structure.

5.6 The application of IL–MOCs in electrochemistry

Electrochemistry is the study of chemical processes that cause electrons to move, it is becoming increasingly important due to its environmental friendliness and profound influence on fields such as materials science, environmental monitoring, and sustainable energy solutions. The utilization of either IL[151] or POM[152] in electrochemistry has gained significant attention due to their unique properties, including high ionic conductivity and reversible redox activity. The hybrid IL–MOCs also serve as promising catalysts and electroactive materials with higher conductivity and better thermostability, capitalizing on the inherent advantages of ILs and MOCs.[153] The study of the $[S_2W_{18}O_{62}]^{4-}$ POM reduction in 12 different ILs with a range of different anions and cations revealed strong solvation and ion-pairing effects between the IL cation and the negatively charged POM reduction products.[154] Both the IL and the POM structures can influence the kinetics and thermodynamics of the electron transfer processes, and this should be considered when employing these promising materials for relevant electrochemical applications.

POM–ILs based on the phosphomolybate anion $[PMo_{12}O_{40}]^{3-}$ and organic imidazolium, pyridinium, and phosphorous cations were prepared and used as electrochromic materials with deep eutectic solvents as electrolytes to design efficient electrochromic devices.[155] Additionally, Mo-based electrodes derived from POM–IL, denoted as N/P-MoO_2@carbon, were designed and exhibited advanced electrochemical performance.[156] The contents of C, N, P, and the pore geometry of N/P-MoO_2@carbon networks can be easily tailored by adjusting the precursor's cyano group position, resulting in enhanced lithium storage performance. Moreover, composite catalysts composed of Pd, POM–IL, and N,P-codoped coal-based carbon fibers have been developed, exhibiting superior activity for formic acid electrooxidation compared to non-enhanced Pd/N, P–C composites.[157] This enhanced performance is attributed to the synergistic effects of the POM anion and the longer alkyl chains in the imidazole IL, leading to smaller catalyst particles and increased active sites being exposed, thus better electrochemical performance.

Furthermore, a Co-based CoW_{12}–IL–graphene oxide system was reported as an efficient electrocatalyst for water oxidation in neutral pH conditions (Scheme 9).[158] This new hybrid material was prepared by covalent attachment of IL species to graphene oxide and then electrostatic interaction of supported imidazolium cations with Keggin type $[CoW_{12}O_{40}]^{6-}$ polya-

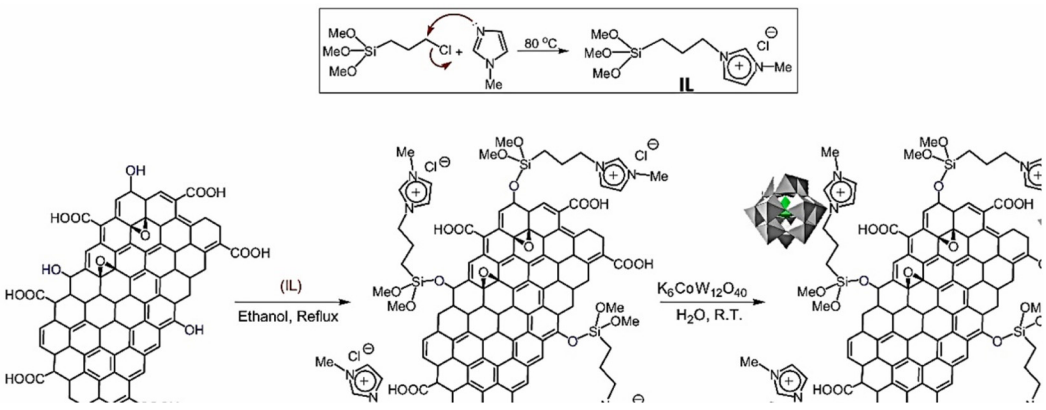

Scheme 9 Schematic exhibition of the preparation of CoW_{12}–IL–graphene oxide hybrid nanomaterial. Adapted from ref. 158 with permission from Elsevier, copyright 2022.

nions, it is the strong electrostatic interaction between imidazolium cations and CoW_{12} species prevents the leaching of catalytically active species into the solution. It exhibited remarkable stability which demonstrated the efficiency and stability of the oxygen evolution reaction process in neutral pH.

Overall, the tunable nature of IL–MOCs allows for precise control over the electrochemical properties, making them suitable for applications such as energy storage devices, sensors, and electrocatalysis. The synergistic effects between the IL environment and the MOCs enhance the stability and conductivity of the electroactive materials, paving the way for advancements in electrochemical technologies with improved efficiency and performance.

6. Conclusion

To gain deep insight into the development of new IL–MOC systems in catalytic application, it's crucial to consider specific aspects such as ease of synthesis, catalytic efficiency, stability, environmental impact, *etc*. The IL–MOC hybrids are easy to prepare *via* anion exchange or simple mixing, offering advantages over traditional ILs or MOCs. Ongoing research focuses on enhancing their structural diversity and functional properties to broaden their applicability across various fields.

ILs can not only stabilize but also regulate MOC structure, reactivity, and catalytic performance. By interacting with MOCs, ILs can alter MOCs' coordination environment, structural arrangement and even oxygen vacancy density. This interaction may lead to changes in the size, shape, and surface properties of MOCs. Additionally, ILs can affect the redox behavior of MOCs by donating or accepting electrons, and they can also modify the acidity, basicity, hydrophilicity or hydrophobicity. Meanwhile, it has been proved that the composition and morphology of MOCs are quite significant factors affecting the catalytic efficiency. Thus ILs can ultimately influence MOCs' catalytic activity and selectivity. Furthermore, ILs provide a unique solvent environment that surrounds MOCs, influencing their solubility, stability, and accessibility to reactants. The solvation effects of ILs can enhance the dispersion of MOCs, increase their surface area, and facilitate the diffusion of reactant molecules to active sites.

IL–MOCs offer higher catalytic efficiency with increased reaction rates, higher selectivity, and overall improved performance in catalytic processes. They also exhibit improved stability due to the high thermal stability and non-volatility characteristics of ILs, allowing for easy separation and better recyclability. Additionally, the versatility and flexibility of IL–MOCs, stemming from ILs' tunability, make them applicable for various types of catalytic reactions, while their green solvent properties reduce environmental impact by simplifying reaction conditions, minimizing waste generation, and lowering overall costs. Moreover, ILs are non-volatile, which means they are less likely to evaporate than traditional solvents. This makes them safer and more attractive to use than traditional solvents, particularly in industrial applications where solvent loss is a concern.

However, there are still some challenges to overcome, such as the cost and availability of ILs, as they are currently more expensive than traditional solvents. Further research is needed to develop new ILs with the desired properties. Additionally, there is still a need for a better understanding of the underlying chemistry of IL–MOCs. Especially, understanding the role of IL in stabilizing/regulating MOCs will foster new discoveries of catalytic reactions that are accelerated by IL–MOC catalysts. This will be essential for developing new and improved IL–MOCs for a wider range of applications. Despite these challenges, IL–MOCs are a promising new class of catalysts with a wide range of potential applications.

In summary, IL–MOCs are a fascinating class of materials with promising catalytic applications. The unique combination of MOCs and ILs brings forth several noteworthy advantages in various chemical transformations. As researchers continue to explore the potential of IL–MOCs, we can anticipate even more remarkable applications in the near future. For example, new IL–MOC combinations could be explored to expand the catalytic scope and improve efficiency. This involves synthesizing and characterizing a diverse range of IL–MOCs to identify promising candidates for various chemical transformations. Meanwhile, detailed mechanistic studies are essential to understand the reaction pathways and active sites involved in IL–MOC catalysis. Techniques such as spectroscopy, microscopy, and computational modeling can provide valuable insights into the fundamental processes occurring at the molecular level, aiding in catalyst design and optimization. Moreover, the stability and recyclability of IL–MOC catalysts could be further enhanced for practical applications and sustainability. Beyond catalytic oxidation reactions, IL–MOCs already offered exciting opportunities for emerging applications such as biomass conversion, CO_2 utilization, and renewable energy storage. Future studies should explore these novel application areas and assess the feasibility and potential impact of IL–MOC catalysis. Although the field of IL–MOC hybrids is still young and there are still some challenges to overcome, the utilization of IL–MOCs is preferable from the viewpoint of both industry and society as they align more closely with the principles of green chemistry.

Abbreviations

IL	Ionic liquid
MOC	Metal oxocluster
IL–MOCs	IL-stabilized metal oxoclusters
PIL	Polymeric ionic liquid
POMs	Polyoxometalates
POM–ILs	POM-based ILs
HPAs	Heteropoly acids
PEG	Polyethylene glycol
[Hbet][NTf_2]	Protonated betaine bis(trifluoromethylsulfonyl)imide
EMIm	1-Ethyl-3-methylimidazolium
BMIm	1-Butyl-3-methylimidazolium

Gr	Graphene
HDIm	Protic *N*-dodecylimidazolium
MNP	Magnetic nanoparticles
BPy	*N*-Butylpyridinium
$P_{4,4,4,n}$	Quaternary phosphonium cation
DMIm	1-Dodecyl-3-methylimidazolium
TTA	Tetradecyl trimethyl ammonium
TBA	Tetrabutylammonium
NH_4–Nb	Ammonium peroxoniobate
Pic	Picolinate ions
Bim	1-Butylimidazolium
MIMPS	Methylimidazolium propyl sulfobetaine
Py	Pyridinium
PyPS	3-(Pyridine-1-ium-1-yl) propane-1-sulfonate
TEAPS	1-(3-Sulfonic group) trimethylamine
Dopy	*N*-*n*-Dodecylpyridinium
Im-PEG-Im	PEG-functionalized alkylimidazolium
C_{12}MIm	1-Dodecyl-3-methylimidazolium
CTA	Cetyltrimethyl-ammonium
ODA	Octadecylmethylammonium
Co_4PW–PDDVAC	A porous POM-based composite
^{t}Bu-Hptz	2-*tert*-Butyl-5-(2-pyridyl)tetrazole
TOMA	Methyltrioctylammonium
PS–IL–PW	$[\alpha\text{-}PW_{12}O_{40}]^{3-}$ Immobilized on IL-modified polystyrene resin beads
CMC	Carboxymethyl cellulose
AIL	Acidic IL
SACs	Single-atom catalysts
POM-SACs	POM-supported SACs
MOFs	Metal–organic frameworks
DEDSA	Diethyldisulphoammonium
BSmIm	$-SO_3H$-functionalized imidazolium cation
$[C_2OHC_1Im]$	1-(Hydroxyethyl)-3-methylimidazole
POMs-ILs@MOFs	MOF encapsulated POMs-based ILs
TON	Turnover number
TOF	Turnover frequency
HPMoV	$H_5PMo_{10}V_2O_{40}$
FA	Formic acid
LA	Levulinic acid
ODS	Oxidative desulfurization
PET	Polyethylene terephthalate
BHET	Bis(hydroxyethyl) terephthalate

Conflicts of interest

There are no conflicts to declare.

Acknowledgements

The authors acknowledge the support from the National Key Research and Development Program of China (2022YFA1504903), State Key Laboratory of Petroleum Molecular & Process Engineering and the National Natural Science Foundation of China (21978095). Y. Qiao would like to thank the financial support by the Max Planck Society.

References

1 S. S. Wang and G. Y. Yang, *Chem. Rev.*, 2015, **115**, 4893–4962.
2 U. Schubert, in *Macromolecules Containing Metal and Metal-Like Elements*, ed. A. S. Abd-El-Aziz, C. E. Carraher Jr., C. U. Pittman Jr. and M. Zeldin, John Wiley & Sons, 2005, ch. 2, vol. 7, pp. 55–71.
3 M. Carraro and S. Gross, *Materials*, 2014, **7**, 3956–3989.
4 C. Wang, J. H. Yan, S. X. Chen and Y. Liu, *ChemPlusChem*, 2023, **88**, e202200462.
5 F. de Azambuja, J. Moons and T. N. Parac-Vogt, *Acc. Chem. Res.*, 2021, **54**, 1673–1684.
6 D. E. Salazar Marcano, N. D. Savić, K. Declerck, S. A. M. Abdelhameed and T. N. Parac-Vogt, *Chem. Soc. Rev.*, 2024, **53**, 84–136.
7 J. W. Zhong, J. Pérez-Ramírez and N. Yan, *Green Chem.*, 2021, **23**, 18–36.
8 D. M. Cheng, K. Li, H. Y. Zang and J. J. Chen, *Energy Environ. Mater.*, 2023, **6**, e12341.
9 A. Misra, I. F. Castillo, D. P. Müller, C. González, S. Eyssautier-Chuine, A. Ziegler, J. M. de la Fuente, S. G. Mitchell and C. Streb, *Angew. Chem., Int. Ed.*, 2018, **57**, 14926–14931.
10 I. Majeed, Z. Ahmad, N. AlMasoud, T. S. Alomar, S. Hussain, H. M. Asif, F. Mansoor, Z. Nazar and Z. M. El-Bahy, *Polyhedron*, 2023, **243**, 116577.
11 C. L. Hill, *J. Mol. Catal. A: Chem.*, 2007, **262**, 2–6.
12 A. Patel, N. Narkhede, S. Singh and S. Pathan, *Catal. Rev.*, 2016, **58**, 337–370.
13 Q. D. Liu and X. Wang, *Matter*, 2020, **2**, 816–841.
14 B. Smarsly and H. Kaper, *Angew. Chem., Int. Ed.*, 2005, **44**, 3809–3811.
15 Y. X. Qiao and Z. S. Hou, *Curr. Org. Chem.*, 2009, **13**, 1347–1365.
16 S. Ivanova, *ISRN Chem. Eng.*, 2014, **2014**, 963792.
17 Y. Martinetto, B. Pégot, C. Roch-Marchal, B. Cottyn-Boitte and S. Floquet, *Eur. J. Inorg. Chem.*, 2020, 228–247.
18 E. Ahmed and M. Ruck, *Angew. Chem., Int. Ed.*, 2012, **51**, 308–309.
19 C. B. Hong, T. Wang and H. C. Liu, *Inorg. Chem.*, 2023, **62**, 4054–4065.
20 A. B. Bourlinos, K. Raman, R. Herrera, Q. Zhang, L. A. Archer and E. P. Giannelis, *J. Am. Chem. Soc.*, 2004, **126**, 15358–15359.
21 X. Z. Li, H. Y. Xue, Q. Lin and A. M. Yu, *Appl. Organomet. Chem.*, 2020, **34**, e5606.
22 S. X. Mao, Q. H. Zhou, H. L. Guo, M. Du, W. S. Zhu, H. M. Li, J. Y. Pang, D. B. Dang and Y. Bai, *Fuel*, 2023, **333**, 126392.
23 H. X. Chen, S. T. Hou, H. Y. Cui, C. Wang, M. Zhang, H. P. Li, H. Xu, J. Q. Wu and W. S. Zhu, *J. Mol. Liq.*, 2023, **379**, 121650.

24 S. Y. Zhang, Q. Zhuang, M. Zhang, H. Wang, Z. M. Gao, J. K. Sun and J. Y. Yuan, *Chem. Soc. Rev.*, 2020, **49**, 1726–1755.
25 P. Nockemann, B. Thijs, S. Pittois, J. Thoen, C. Glorieux, K. Van Hecke, L. Van Meervelt, B. Kirchner and K. Binnemans, *J. Phys. Chem. B*, 2006, **110**, 20978–20992.
26 P. Nockemann, B. Thijs, K. V. Hecke, L. V. Meervelt and K. Binnemans, *Cryst. Growth Des.*, 2008, **8**, 1353–1363.
27 P. G. Rickert, M. R. Antonio, M. A. Firestone, K.-A. Kubatko, T. Szreder, J. F. Wishart and M. L. Dietz, *Dalton Trans.*, 2007, **5**, 529–531.
28 P. G. Rickert, M. R. Antonio, M. A. Firestone, K.-A. Kubatko, T. Szreder, J. F. Wishart and M. L. Dietz, *J. Phys. Chem. B*, 2007, **111**, 4685–4692.
29 S. W. Lin, W. L. Chen, Z. M. Zhang, W. L. Liu and E. B. Wang, *Acta Crystallogr., Sect. E: Struct. Rep. Online*, 2008, **E64**, m954.
30 S. W. Lin, W. L. Liu, Y. G. Li, Q. Wu, E. B. Wang and Z. M. Zhang, *Dalton Trans.*, 2010, **39**, 1740–1744.
31 S. L. Linguito, X. Zhang, M. Padmanabhan, A. V. Biradar, T. T. Xu, T. J. Emge, T. Asefa and J. Li, *New J. Chem.*, 2013, **37**, 2894–2901.
32 T. L. Greaves and C. J. Drummond, *Chem. Soc. Rev.*, 2008, **37**, 1709–1726.
33 H. W. Yang, L. J. Bai, D. L. Wei, L. X. Yang, W. X. Wang, H. Chen, Y. Z. Niu and Z. X. Xue, *Chem. Eng. J.*, 2019, **358**, 850–859.
34 Z. K. Guan, M. M. Wang, G. X. Sun, X. Xue, Y. F. Chen, Y. Zhang, T. Zhao, H. F. Shi, C. Feng, Y. Pan and Y. Q. Liu, *Fuel*, 2024, **357**, 129887.
35 Y. T. Gao, M. Choudhari, G. K. Such and C. Ritchie, *Chem. Sci.*, 2022, **13**, 2510–2527.
36 Z. H. Ma, J. H. Zhang, H. Q. Zhan, M. Xu, H. W. Yang, L. X. Yang, L. J. Bai, H. Chen, D. L. Wei and W. X. Wang, *Process Saf. Environ. Prot.*, 2020, **140**, 26–33.
37 A. Misra, K. Kozma, C. Streb and M. Nyman, *Angew. Chem., Int. Ed.*, 2020, **59**, 596–612.
38 T. V. Marinho, E. Schreiber, R. E. Garwick, W. W. Brennessel and E. M. Matson, *Inorg. Chem.*, 2023, **62**, 15616–15626.
39 P. F. Ji, Y. Song, T. Drake, S. S. Veroneau, Z. K. Lin, X. D. Pan and W. B. Lin, *J. Am. Chem. Soc.*, 2018, **140**, 433–440.
40 U. Schubert, *Coord. Chem. Rev.*, 2017, **350**, 61–67.
41 A. Banerjee, R. Theron and R. W. J. Scott, *ChemSusChem*, 2012, **5**, 109–116.
42 K. Kumari, P. Singh and G. K. Mehrotra, in *Advanced Energy Materials*, ed. A. Tiwari and S. Valyukh, John Wiley & Sons, 2014, pp. 529–553.
43 S. P. Ding, Y. L. Guo, M. J. Hülsey, B. Zhang, H. Asakura, L. M. Liu, Y. Han, M. Gao, J.-y. Hasegawa, B. T. Qiao, T. Zhang and N. Yan, *Chem*, 2019, **5**, 3207–3219.
44 P. Wasserscheid and W. Keim, *Angew. Chem., Int. Ed.*, 2000, **39**, 3772–3789.
45 R. D. Rogers and K. R. Seddon, *Science*, 2003, **302**, 792–793.
46 J. Dupont and J. D. Scholten, *Chem. Soc. Rev.*, 2010, **39**, 1780–1804.
47 Y. X. Qiao, Z. S. Hou, H. Li, Y. Hu, B. Feng, X. R. Wang, L. Hua and Q. F. Huang, *Green Chem.*, 2009, **11**, 1955–1960.
48 Y. X. Qiao, H. Li, L. Hua, L. Orzechowski, K. Yan, B. Feng, Z. Pan, N. Theyssen, W. Leitner and Z. S. Hou, *ChemPlusChem*, 2012, **77**, 1128–1138.
49 J. Z. Chen, L. Hua, C. Chen, L. Guo, R. Zhang, A. J. Chen, Y. H. Xiu, X. R. Liu and Z. S. Hou, *ChemPlusChem*, 2015, **80**, 1029–1037.
50 J. Z. Chen, C. Chen, R. Zhang, L. Guo, L. Hua, A. J. Chen, Y. H. Xiu, X. R. Liu and Z. S. Hou, *RSC Adv.*, 2015, **5**, 25904–25910.
51 D. Liu, J. Z. Gui, F. Lu, Z. L. Sun and Y.-K. Park, *Catal. Lett.*, 2012, **142**, 1330–1335.
52 Y. Martinetto, B. Pégot, C. Roch-Marchal, M. Haouas, B. Cottyn-Boitte, F. Camerel, J. Jeftic, D. Morineau, E. Magnier and S. Floquet, *New J. Chem.*, 2021, **45**, 9751–9755.
53 Y. Martinetto, S. Basset, B. Pégot, C. Roch-Marchal, F. Camerel, J. Jeftic, B. Cottyn-Boitte, E. Magnier and S. Floquet, *Molecules*, 2021, **26**, 496.
54 A. de Zordo-Banliat, K. Grollier, N. Vanthuyne, S. Floquet, T. Billard, G. Dagousset, B. Pégot and E. Magnier, *Angew. Chem., Int. Ed.*, 2023, **62**, e202300951.
55 C. Chen, X. G. Zhao, J. Z. Chen, L. Hua, R. Zhang, L. Guo, B. N. Song, H. M. Gan and Z. S. Hou, *ChemCatChem*, 2014, **6**, 3231–3238.
56 C. Chen, H. Y. Yuan, H. F. Wang, Y. F. Yao, W. B. Ma, J. Z. Chen and Z. S. Hou, *ACS Catal.*, 2016, **6**, 3354–3364.
57 W. B. Ma, H. Y. Yuan, H. F. Wang, Q. Q. Zhou, K. Kong, D. F. Li, Y. F. Yao and Z. S. Hou, *ACS Catal.*, 2018, **8**, 4645–4659.
58 Q. Q. Zhou, M. Ye, W. B. Ma, D. F. Li, B. J. Ding, M. Y. Chen, Y. F. Yao, X. Q. Gong and Z. S. Hou, *Chem. – Eur. J.*, 2019, **25**, 4206–4217.
59 Q. Q. Zhou, B. B. Xu, X. Tang, S. Dai, B. J. Ding, D. F. Li, A. N. Zheng, T. Zhang, Y. F. Yao, X. Q. Gong and Z. S. Hou, *Langmuir*, 2021, **37**, 8190–8203.
60 B. J. Ding, R. Zhang, Q. Q. Zhou, W. B. Ma, A. N. Zheng, D. F. Li, Y. F. Yao and Z. S. Hou, *Mol. Catal.*, 2021, **500**, 111342.
61 W. B. Ma, C. Chen, K. Kong, Q. F. Dong, K. Li, M. M. Yuan, D. F. Li and Z. S. Hou, *Chem. – Eur. J.*, 2017, **23**, 7287–7296.
62 W. B. Ma, Y. X. Qiao, N. Theyssen, Q. Q. Zhou, D. F. Li, B. J. Ding, D. Q. Wang and Z. S. Hou, *Catal. Sci. Technol.*, 2019, **9**, 1621–1630.
63 Q. Q. Zhou, R. Zhang, D. F. Li, B. J. Ding, A. N. Zheng, Y. F. Yao, X. Q. Gong and Z. S. Hou, *Catal. Sci. Technol.*, 2020, **10**, 7601–7612.
64 Y. J. Wang, B. J. Ding, J. J. He, Z. J. Ding and Z. S. Hou, *Energy Fuels*, 2023, **37**, 5429–5440.
65 T. Zhang, X. J. Chen, B. J. Ding, Z. J. Ding, Y. J. Wang, H. W. Qiu, Y. J. Jiang, S. Dai and Z. S. Hou, *Energy Fuels*, 2022, **36**, 1402–1416.

66 Y. Leng, J. Wang, D. R. Zhu, X. Q. Ren, H. Q. Ge and L. Shen, *Angew. Chem., Int. Ed.*, 2009, **48**, 168–171.
67 L. L. Liu, C. C. Chen, X. F. Hu, T. Mohamood, W. H. Ma, J. Lin and J. C. Zhao, *New J. Chem.*, 2008, **32**, 283–289.
68 S. S. Wang, W. Liu, Q. X. Wan and Y. Liu, *Green Chem.*, 2009, **11**, 1589–1594.
69 N. Kashyap, S. Das and R. Borah, *Polyhedron*, 2021, **196**, 114993.
70 D. Liang, N. Zhu, H. L. Zhu, Z. Y. Hu, D. L. Cao and N. Sang, *Catal. Commun.*, 2016, **79**, 49–52.
71 P. B. Hao, M. J. Zhang, W. Zhang, Z. Y. Tang, N. Luo, R. Tan and D. H. Yin, *Catal. Sci. Technol.*, 2018, **8**, 4463–4473.
72 H. Li, Y. X. Qiao, L. Hua, Z. S. Hou, B. Feng, Z. Y. Pan, Y. Hu, X. R. Wang, X. G. Zhao and Y. Yu, *ChemCatChem*, 2010, **2**, 1165–1170.
73 H. Li, Z. S. Hou, Y. X. Qiao, B. Feng, Y. Hu, X. R. Wang and X. G. Zhao, *Catal. Commun.*, 2010, **11**, 470–475.
74 B. S. Chhikara, R. Chandra and V. Tandon, *J. Catal.*, 2005, **230**, 436–439.
75 X. X. Han, K. Ouyang, C. H. Xiong, X. J. Tang, Q. Chen, K. W. Wang, L. L. Liu, C.-T. Hung and S.-B. Liu, *Appl. Catal., A*, 2017, **543**, 115–124.
76 L. Hua, Y. X. Qiao, H. Li, B. Feng, Z. Y. Pan, Y. Y. Yu, W. W. Zhu and Z. S. Hou, *Sci. China: Chem.*, 2011, **54**, 769–773.
77 L. Hua, Y. X. Qiao, Y. Y. Yu, W. W. Zhu, T. Cao, Y. Shi, H. Li, B. Feng and Z. S. Hou, *New J. Chem.*, 2011, **35**, 1836–1841.
78 L. Jing, J. Shi, F. M. Zhang, Y. J. Zhong and W. D. Zhu, *Ind. Eng. Chem. Res.*, 2013, **52**, 10095–10104.
79 J. L. Xu, H. Y. Zhang, Y. F. Zhao, Z. Z. Yang, B. Yu, H. J. Xu and Z. M. Liu, *Green Chem.*, 2014, **16**, 4931–4935.
80 J. W. Zhang, X. Y. Zhu, X. X. Xu, Q. Q. Sun, L. G. Wei, K. L. Li, S. R. Zhai and Q. D. An, *J. Environ. Chem. Eng.*, 2022, **10**, 108260.
81 K. X. Li, L. L. Bai, P. N. Amaniampong, X. L. Jia, J.-M. Lee and Y. H. Yang, *ChemSusChem*, 2014, **7**, 2670–2677.
82 S. Xue, G. J. Chen, Z. Y. Long, Y. Zhou and J. Wang, *RSC Adv.*, 2015, **5**, 19306–19314.
83 Z. B. Liao, Y. L. Duan, L. Y. Guo, R. R. Zheng, L. Y. Wang, Y. M. Chen, L. N. Zhang and X. Qian, *New J. Chem.*, 2023, **47**, 4337–4345.
84 Z. Z. Jiang, H. Y. Wang, L. N. Shan, R. R. Zheng, X. D. Zhao, Z. B. Liao and L. Y. Guo, *Catal. Lett.*, 2023, **153**, 1308–1318.
85 J. X. Yang, N. Chu and X. W. Chen, *Molecules*, 2023, **28**, 3307.
86 T. M. A. Bakker, S. Mathew and J. N. H. Reek, *Sustainable Energy Fuels*, 2019, **3**, 96–100.
87 M. S. Nunes, A. C. Gomes, P. Neves, R. F. Mendes, F. A. A. Paz, A. D. Lopes, M. Pillinger, I. S. Gonçalves and A. A. Valente, *Catal. Today*, 2023, **423**, 114273.
88 Y. Ma, Y. J. Jiang, X. J. Wei, Q. P. Peng, S. Dai and Z. S. Hou, *ACS Sustainable Chem. Eng.*, 2022, **10**, 15389–15401.
89 Y. Ma, C. Chen, Y. J. Jiang, X. J. Wei, Y. Liu, H. Y. Liao, H. F. Wang, S. Dai, P. F. An and Z. S. Hou, *ACS Catal.*, 2023, **13**, 10295–10308.
90 X. J. Lang, Z. Li and C. G. Xia, *Synth. Commun.*, 2008, **38**, 1610–1616.
91 S. Abednatanzi, K. Leus, P. G. Derakhshandeh, F. Nahra, K. De Keukeleere, K. Van Hecke, I. Van Driessche, A. Abbasi, S. P. Nolan and P. V. Der Voort, *Catal. Sci. Technol.*, 2017, **7**, 1478–1487.
92 L. Hua, J. Z. Chen, C. Chen, W. W. Zhu, Y. Y. Yu, R. Zhang, L. Guo, B. N. Song, H. M. Gan and Z. S. Hou, *New J. Chem.*, 2014, **38**, 3953–3959.
93 S. W. Li, R. J. Lou, R. N. Biboum, B. Lepoittevin, G. J. Zhang, A. Dolbecq, P. Mialane and B. Keita, *Eur. J. Inorg. Chem.*, 2013, 1882–1889.
94 R. J. Liu, S. W. Li, G. J. Zhang, A. Dolbecq, P. Mialane and B. Keita, *J. Cluster Sci.*, 2014, **25**, 711–740.
95 W. L. Xie and F. Wan, *Chem. Eng. J.*, 2019, **365**, 40–50.
96 M. M. Jin, Q. T. Niu, G. D. Liu, Z. G. Lv, C. D. Si and H. Y. Guo, *J. Mater. Sci.*, 2020, **55**, 8199–8210.
97 H. Y. Zhao, Y. Z. Li, J. W. Zhao, L. Wang and G. Y. Yang, *Coord. Chem. Rev.*, 2021, **443**, 213966.
98 Y. Y. Li, X. F. Wu, Q. Y. Wu, H. Ding and W. F. Yan, *Ind. Eng. Chem. Res.*, 2014, **53**, 12920–12926.
99 R. J. Liu and C. Streb, *Adv. Energy Mater.*, 2021, **11**, 2101120.
100 X. J. Wei, Y. J. Jiang, Y. Ma, J. Fang, Q. B. Peng, W. Xu, H. Y. Liao, F. X. Zhang, S. Dai and Z. S. Hou, *Chem. – Eur. J.*, 2022, **28**, e202200374.
101 G. D. Yadav, R. K. Mewada, D. P. Wagh and H. G. Manyar, *Catal. Sci. Technol.*, 2022, **12**, 7245–7269.
102 J. Liu, Y. Liu, Y. Liu, Y. Wang, F. Q. Wu, Z. Zhou and Z. B. Zhang, *ACS Sustainable Chem. Eng.*, 2023, **11**, 12934–12945.
103 N. Sun, X. Y. Jiang, M. L. Maxim, A. Metlen and R. D. Rogers, *ChemSusChem*, 2011, **4**, 65–73.
104 H. Y. Deng, W. B. B. Xu, D. Zhang, X. Y. Li and J. Y. Shi, *Polymers*, 2023, **15**, 2401.
105 J. A. Abia and R. Ozer, *BioResources*, 2013, **8**, 2924–2933.
106 G. F. De Gregorio, R. Prado, C. Vriamont, X. Erdocia, J. Labidi, J. P. Hallett and T. Welton, *ACS Sustainable Chem. Eng.*, 2016, **4**, 6031–6036.
107 X. Xin, Z. Li, M. Z. Chi, M. Zhang, Y. Y. Dong, H. J. Lv and G. Y. Yang, *Green Chem.*, 2023, **25**, 2815–2824.
108 K. X. Li, L. Z. Huang, Y. Zhang, Z. T. Zhu, J. Zhao, G. J. Xia and Y. G. Min, *Ind. Eng. Chem. Res.*, 2023, **62**, 18337–18349.
109 Z. H. Li, Y. M. Li, Y. N. Chen, Q. W. Wang, M. Jadoon, X. H. Yi, X. Z. Duan and X. H. Wang, *ACS Catal.*, 2022, **12**, 9213–9225.
110 Z. P. Cai, J. X. Long, Y. W. Li, L. Ye, B. L. Yin, L. J. France, J. C. Dong, L. R. Zheng, H. Y. He, S. J. Liu, S. C. E. Tsang and X. H. Li, *Chem*, 2019, **5**, 2365–2377.
111 Z. P. Cai, R. J. Chen, H. Zhang, F. K. Li, J. X. Long, L. L. Jiang and X. H. Li, *Green Chem.*, 2021, **23**, 10116–10122.

112 Z. Wu, L. Hu, Y. T. Jiang, X. Y. Wang, J. X. Xu, Q. F. Wang and S. F. Jiang, *Biomass Convers. Biorefin.*, 2023, **13**, 519–539.
113 Y. C. Hou, M. G. Niu and W. Z. Wu, *Ind. Eng. Chem. Res.*, 2020, **59**, 16899–16910.
114 F. Boshagh, M. Rahmani, K. Rostami and M. Yousefifar, *Energy Fuels*, 2022, **36**, 98–132.
115 M. Haghighi and S. Gooneh-Farahani, *Environ. Sci. Pollut. Res.*, 2020, **27**, 39923–39945.
116 F. Liu, J. Yu, A. B. Qazi, L. Zhang and X. K. Liu, *Environ. Sci. Technol.*, 2021, **55**, 1419–1435.
117 J. R. Li, Z. Yang, S. W. Li, Q. P. Jin and J. S. Zhao, *J. Ind. Eng. Chem.*, 2020, **82**, 1–16.
118 X. B. Lim and W.-J. Ong, *Nanoscale Horiz.*, 2021, **6**, 588–633.
119 M. Ahmadian and M. Anbia, *Energy Fuels*, 2021, **35**, 10347–10373.
120 H. Liu, H. Xu, M. Hua, L. Chen, Y. Wei, C. Wang, P. Wu, F. Zhu, X. Chu, H. Li and W. Zhu, *Fuel*, 2020, **260**, 116200.
121 J. Wang, B. Yang, X. L. Peng, Y. C. Ding, S. S. Yu, F. Q. Zhang, L. F. Zhang, H. D. Wu and J. Guo, *Chem. Eng. J.*, 2022, **429**, 132446.
122 X. X. Xing, H. L. Guo, T. M. He, X. An, H. P. Li, W. S. Zhu, H. M. Li, J. Y. Pang, D. B. Dang and Y. Bai, *ACS Sustainable Chem. Eng.*, 2022, **10**, 11533–11543.
123 Y. Z. Wang, Z. Z. Li, Z. W. Liu and X. Y. Shi, *J. Mol. Liq.*, 2023, **373**, 121245.
124 Y. Gao, L. Cheng, R. Gao, G. Hu and J. Zhao, *J. Hazard. Mater.*, 2021, **401**, 123267.
125 F. Mohammadi-Nejati and S. Shahhosseini, *Fuel Process. Technol.*, 2023, **252**, 107980.
126 H. Ge, Y. Leng, F. Zhang, C. Zhou and J. Wang, *Catal. Lett.*, 2008, **124**, 250–255.
127 Y. Leng, J. Wang, D. Zhu, L. Shen, P. Zhao and M. Zhang, *Chem. Eng. J.*, 2011, **173**, 620–626.
128 P. Zhao, J. Wang, G. Chen, Y. Zhou and J. Huang, *Catal. Sci. Technol.*, 2013, **3**, 1394–1404.
129 P. Zhao, Y. Leng and J. Wang, *Chem. Eng. J.*, 2012, **204–206**, 72–78.
130 P. Zhao, Y. Zhou, Y. Liu and J. Wang, *Chin. J. Catal.*, 2013, **34**, 2118–2124.
131 Z. Long, Y. Zhou, W. Ge, G. Chen, J. Xie, Q. Wang and J. Wang, *ChemPlusChem*, 2014, **79**, 1590–1596.
132 X. Cai, Q. Wang, Y. Liu, J. Xie, Z. Long, Y. Zhou and J. Wang, *ACS Sustainable Chem. Eng.*, 2016, **4**, 4986–4996.
133 Z. Long, Y. Zhang, G. Chen, J. Shang, Y. Zhou, J. Wang and L. Sun, *ACS Sustainable Chem. Eng.*, 2019, **7**, 4230–4238.
134 C. Yuan, X. Gao, Z. Pan, X. Li and Z. Tan, *Catal. Commun.*, 2015, **58**, 215–218.
135 M. Taheri, M. Ghiaci, A. Moheb and A. Shchukarev, *Appl. Organomet. Chem.*, 2019, **33**, e5012.
136 H. Wang, L. Fang, Y. Yang, L. Zhang and Y. Wang, *Catal. Sci. Technol.*, 2016, **6**, 8005–8015.
137 H. Han, T. Jiang, T. Wu, D. Yang and B. Han, *ChemCatChem*, 2015, **7**, 3526–3532.
138 P. T. Fang, B. Liu, J. L. Xu, Q. Zhou, S. J. Zhang, J. Y. Ma and X. M. Lu, *Polym. Degrad. Stab.*, 2018, **156**, 22–31.
139 P. T. Fang, X. Zheng, R. Q. Zhang, J. L. Xu, D. X. Yan, Q. Zhou, J. Y. Xin, C. Y. Shi, S. Q. Xia and X. M. Lu, *ChemCatChem*, 2023, **15**, e202200712.
140 M. Y. Wang, R. Ma and L. N. He, *Sci. China: Chem.*, 2016, **59**, 507–516.
141 M. Y. Wang and X. B. Ma, in *Encyclopedia of Ionic Liquids*, ed. S. J. Zhang, Springer, Singapore, 2019. DOI: **10.1007/978-981-10-6739-6_35-2**.
142 Y. Ma, X. J. Wei, J. Fang, Q. B. Peng, W. Xu and Z. S. Hou, *Green Chem. Eng.*, 2022, **3**, 146–156.
143 A. Patel, J. Patel and S. Pathan, *Inorg. Chem.*, 2023, **62**, 6970–6980.
144 M. A. Alotaibi, E. F. Kozhevnikova and I. V. Kozhevnikov, *Chem. Commun.*, 2012, **48**, 7194–7196.
145 B. Zhang, G. Sun, S. P. Ding, H. Asakura, J. Zhang, P. Sautet and N. Yan, *J. Am. Chem. Soc.*, 2019, **141**, 8185–8197.
146 S. J. Li, Y. B. Ma, Y. Zhao, R. J. Lou, Y. P. Zhao, X. S. Dai, N. N. Ma, C. Streb and X. N. Chen, *Angew. Chem., Int. Ed.*, 2023, **62**, e202314999.
147 X. J. Wei, Y. J. Jiang, Y. Ma, H. Y. Liao, S. Dai, P. F. An, Z. Q. Wang, X. Q. Gong and Z. S. Hou, *ACS Catal.*, 2024, **14**, 5344–5355.
148 A. Modvig, C. Kumpidet, A. Riisager and J. Albert, *Materials*, 2019, **12**, 2175.
149 Q. B. Peng, X. G. Zhao, M. Y. Chen, J. J. Wang, K. Cui, X. J. Wei and Z. S. Hou, *Mol. Catal.*, 2022, **517**, 112049.
150 Z. R. Zhang, M. Y. Liu, J. L. Song, H. Z. Liu, Z. B. Xie, S. S. Liu, Q. L. Meng, P. Zhang and B. X. Han, *Green Chem.*, 2018, **20**, 4865–4869.
151 M. Armand, F. Endres, D. R. MacFarlane, H. Ohno and B. Scrosati, *Nat. Mater.*, 2009, **8**, 621–629.
152 T. Ueda, *ChemElectroChem*, 2018, **5**, 823–838.
153 Z. Q. Wang, L. M. Ai, X. S. Lv, Z. J. Wang, F. W. He and Q. Y. Wu, *Int. J. Electrochem. Sci.*, 2020, **15**, 223–230.
154 J. I. Phillips, S. Azuma, J. Lee, T. Ueda and D. S. Silvester, *Aust. J. Chem.*, 2022, **75**, 865–876.
155 H. Cruz, N. Gomes, F. Mirante, S. S. Balula, L. C. Branco and S. Gago, *ChemistrySelect*, 2020, **5**, 12266–12271.
156 G. J. Chen, L. Zhang, Y. D. Zhang, K. Liu, Z. Y. Long and Y. Wang, *J. Mater. Chem. A*, 2019, **7**, 7194–7201.
157 M. R. Lou, R. Y. Wang, L. L. Yang, D. Z. Jia, Z. P. Sun, L. X. Wang, Y. Guo, X. C. Wang, J. Zhang and H. L. Shi, *Appl. Surf. Sci.*, 2020, **516**, 146137.
158 S. Shahsavarifar, M. Masteri-Farahani and M. R. Ganjali, *Colloids Surf., A*, 2022, **632**, 127812.